UNIVERSITY OF PRETORIA

Department of Physics

THE DESIGN AND EVALUATION OF AN ATHERMAL LASER BEAM EXPANDER

by

A. E. Reitmann

Submitted as part of the requirements of the

M.Sc. Degree in Physics

May 1987

ABSTRACT

A systematic design procedure for a laser beam expander is given in which special emphasis is placed on the athermalization process during the predesign stage.

Initially the aberration theory, as well as the theory of athermalization and a functional model for simulating a Nd-Yag laser are presented. These theories are consequently used in the design of the beam expander.

The design process starts off by translating the user requirements into optical design specifications. These specifications were used as a basis for the design of a two lens athermalized system which was corrected for aberrations. Unfortunatly, the resultant design could not entirely meet the user requirements, and a more complex design was indicated.

A three lens system was then assumed which required a completely new approach to athermalization and aberration correction. Four equations, expressing magnification, total length, afocality and atermalization were simultaneously solved and gave a first order layout. The aberrations were then minimized and the final design realized.

The final design was evaluated and the results compared with

specifications. For the analysis the expected radiation pattern of the complete laser/beam expander system was constructed and the relationship between the uniformity of the radiation pattern and the exit pupil diameter was established. The analysis shows conclusively that the design is optimal and that it satisfies all user requirements.

CONTENTS.

CHAPTER 1

1 ATHERMAL LASER BEAM EXPANDER

1.1 INTRODUCTION

A laser beam expander was designed for a hand-held laser target designator and rangefinder. The beam expander had to reduce the inherent divergence of a given Nd-Yag laser. The beam expander had to be light and rugged and be uneffected by operational environmental conditions.

A similar beam expander had been designed by the C.S.I.R.[1]. In their design report it was pointed out that a serious degradation in the performance of the beam expander takes place as a result of a change in temperature.

The aim during the design of the beam expander presented in this thesis was to athermalize the beam expander. The design would thus be assembled in a laboratory and should then preserve its performance and remain uneffected by operational environmental conditions such as temperature changes.

In chapter 2 of this report the theoretical background required to perform the design is briefly presented. The specifications

to which the beam expander was designed are derived and summarized in chapter 3. Chapter 4 presents the conceptual design of a two lens system which could not entirely meet the required performance. The conceptual design of a three lens beam expander which satisfies all the requirements is presented in chapter 5. The performance of this design is evaluated in chapter 6. In conclusion some remarks regarding the uniformity of the far-field intensity distribution of the complete beam expander are made in chapter 7.

CHAPTER 2

2 THEORETICAL BACKGROUND.

This section briefly deals with the theory of the equations which are used in the design of the beam expander.

In order to meet the divergence specification (presented in chapter 3) the performance of the beam expander had to be closely controlled. Since the optical performance is quantified in terms of the aberrations of the system, the underlying theory of the applicable aberrations is presented:

2.1 ABERRATION THEORY.

2.1.1 IDEAL OPTICAL SYSTEMS.

An ideal optical system is a theoretical abstraction which produces perfect optical images[2]. Deviations from producing perfect images are termed aberrations.

2.1.2 ABERRATIONS.

The aberrations of an optical system can be determined by finite ray tracing. This method is however mainly useful for evaluation of existing optical systems and hardly suitable for the synthesis of new systems. The problem then, from an optical designers point of view, is to design an optical system in which the aberrations are small enough in order to meet a given set of tolerances. To achieve this, a thorough knowledge of how the aberrations arise and how they are related to the physical structure of a lens is required.

The first step to realize this is to identify and classify different types of aberrations. This challenge was taken up by many scientists such as Buchdahl[3], Hamilton[4], Born and Wolf[5] etc. These scientists classified aberrations according to the dependence of the aberration on pupil and field coordinates and in the wavelength of the light being transmitted through the optical system.

All aberrations were classified into three main groups i.e.

1) Monochromatic aberrations
2) Chromatic aberrations
3) Chromatic variations of monochromatic aberrations.

Since the beam expander is illuminated by virtually monochromatic light no derivation of wavelength dependent aberrations is presented in this thesis. The theory of monochromatic aberrations follows:

2.1.3 MONOCHROMATIC WAVEFRONT AND TRANSVERSE RAY ABERRATIONS.

The wavefront aberrations of an optical system can be defined as follows[2]:

Let O in fig 2.1 be the centre of the exit pupil of a symmetrical optical system and let OP'$_o$ be a principal ray from an object point P, not shown. Let X and Y be mutually perpendicular axes in the pupil and let X' and Y' be axes in the image plane. Since the optical system is rotationally symmetric, chose P to be in the YZ plane. Let S' be the wavefront from P through O and S a spherical reference sphere with centre P'$_o$ and radius OP'$_o$. Let a ray r' from P meet S and S' at Q$_o$(x_o,y_o,z_o) and Q(x,y,z) and the image plane at P'(x',y') respectively. The coordinate of P'$_o$ is (0,y'$_o$).

The wavefront aberration W is defined as the optical path difference between Q$_o$ and Q and is due to the non-sphericity of the emerging wavefront. The wavefront aberration W is a function of x, y and y'. Due to symmetry considerations it can be shown that [2] $W=W(x^2+y^2 , yy', y'^2)$

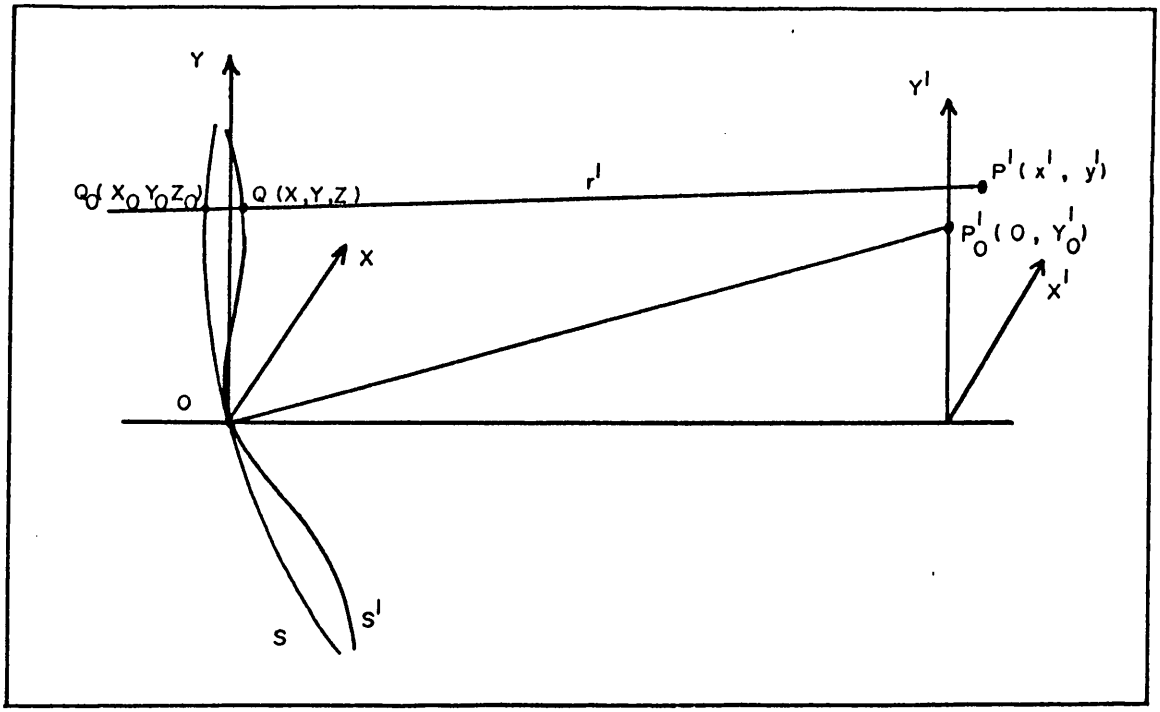

FIG 2.1 Wavefront and transverse ray aberrations

The transverse ray aberration is defined as the distance between P'$_0$ and P' and can be decomposed into two mutually perpendicular components : the tangential, TRA(y) and radial, TRA(x) transverse ray aberrations.

The transverse ray aberrations and wavefront aberrations are linked by the following equation

$$(2.1) \qquad TRA(y) = -\frac{R}{n}\frac{\partial W}{\partial y}$$

$$(2.2) \qquad TRA(x) = -\frac{R}{n}\frac{\partial W}{\partial x}$$

where R is the radius of the reference sphere.

These equations hold true for the Seidel region only.

2.1.4 CLASSIFICATION OF MONOCHROMATIC ABERATIONS.

As mentioned above the wavefront aberrations of a symmetrical optical system are functions of x^2+y^2 , yy' and y'^2 . They can therefore be expressed as a power series of these variables, thus:

$$(2.3) \qquad W = W(x^2+y^2, yy', y'^2)$$
$$= A1(x^2+y^2) + A2(yy') + A3(y'^2)$$
$$+ B1(x^2+y^2)^2 + B2(x^2+y^2)yy' + B3(yy')^2$$
$$+ B4(x^2+y^2)y'^2 + B5(yy'^3) + B6(y'^4)$$
$$+ \text{terms of order 6 and higher.}$$

The constant term in the expression vanishes because both the real and reference wavefronts intersect the pupil in O. Furthermore, all the terms independent of pupil variables also vanish because the wavefront aberration cannot be independent of the pupil variables.

The remaining second order terms are $A1(x^2+y^2)$ and $A2yy'$.

These terms can be assosiated with defocussing. The first term, $A1(X^2 + Y^2)$ is a longitudinal defocussing. Since P'$_o$ was chosen to be in the Gaussian image plane, the coefficient A1 is zero. The second term A2yy' is a transverse shift of the centre of the reference sphere relative to the Gaussian image point. Again, since P'$_o$ and the Gaussian image point are chosen to coincide, the coefficient A2 is also zero.

The remaining fourth degree terms in the wavefront expansion expression, eq.2.3 are:

$B1(x^2+y^2)^2$

$B2(x^2+y^2)yy'$

$B3(yy')^2$

$B4(x^2+y^2)y'^2$ and

$B5yy'^3$ and they are known as primary, Seidel or third order aberrations. These aberrations are called "Seidel" aberrations, after L. Seidel[2], who developed the first explicit systematical formulae for computing them. The Seidel aberrations are unique and all the different methods of computing them lead essentially to the same quantities[2]. This can not be said of the higher order aberrations, since the classification of higher order aberrations are dependent on the choice of references and variables.

A laser beam expander will generally operate at very small field angles and the field dependent aberrations will

therefore be negligible. The only relevant Seidel aberration in the design of the beam expander is thus the term $B1(x^2+y^2)^2$, also known as third order spherical aberration. This aberration will be discussed in some detail below.

2.1.5 CALCULATION OF SPHERICAL ABERRATION.

The Seidel aberrations of an optical system can[6] be decomposed into the individual surface contributions, which may be added up to yeild the total aberration in question. The magnitude of the individual surface contributions of each Seidel aberration are linked to the constructional parameters and conjugates of the optical system and are indicative of how active a particular surface is. This method of analysis allows one to manipulate aberrations[2] in a direct and predetermined manner.

The wavefront aberration introduced by the third order spherical aberration, expressed as a summation of the individual surface contributions, is given by the following expression[2].

(2.4) $$W(x,y,y') = 1/8[\ -\Sigma A^2 h\triangle(u/n)\ ](x^2+y^2)^2/h'^4$$

$$= 1/8[\ S_1\ ](x^2+y^2)^2/h'^4$$

where A is the refraction invariant of the

marginal ray,
h is the height at which the marginal ray strikes the surface,
h' is the height of the marginal ray in the pupil of the system,
u is the paraxial angle of the marginal ray,
n is the refractive index,
x and y are the coordinates of the marginal ray in the pupil.

S_1 is the third order spherical aberration coefficient which is obtained by the process of summation over all the surfaces of the system, as indicated in equation 2.4.

This equation shows a strong resemblance to the term $B1(X^2+Y^2)^2$ in equation 2.3.

Equation 2.4 can be applied to determine to what extent the different surfaces contribute to the total spherical aberration, by simply tracing the paraxial marginal ray from the axial object point through the rim of the pupil.

2.1.6 THIN LENS SPHERICAL ABERRATION.

A thin lens[7] is a lens which has no axial thickness. The principal points, the optical centre and the vertices of the two optical surfaces are therefore coincident. Since the concept of thin lenses significantly simplifies the analytical treatment of aberrations it is extensively used in this thesis.

The third order spherical aberration of a thin lens is a function of the shape of the lens and of the conjugates at which the lens is used. M.J.Kidger [7] defined a shape factor (or bending) B, and a conjugate variable C of a thin lens as follows:

(2.5) $B = h(c_1 + c_2)$

where h is the height at which the marginal ray strikes the lens
and ci is the curvature of the i-th optical active surface

(2.6) $C = u + u'$

where u and u' are the paraxial angles of the marginal ray entering and exiting the lens respectively.

The third order spherical aberration of thin lenses are given by[7]:

(2.7) $S_1 = (Kh^2/4n'^2)[(hKn/n-1)^2 + (n+2)/n\ (B+C)^2 + 2C(B+C)]$

where $K = n'(n-1)[c_1 - c_2]$ = power of a thin lens

n = the refractive index of the lens relative to that of air

n'= the refractive index of the medium surrounding the lens.

The third order spherical aberration of more than one lens can simply be added to obtain the total third order spherical aberration of a complete optical system. This property was used during the predesign of the beam expander.

2.2 THEORY OF ATHERMALIZATION.

One of the aims during the design of the beam expander was to athermalize the beam expander. The effect of temperature changes on thin lens systems thus needs to be quantified. The theory is presented below:

2.2.1 THERMAL EFFECTS IN OPTICAL SYSTEMS.

Past experience[1] has shown that the performance of optical systems can adversely be changed when subjected to changes in temperature. The resulting performance degradation is mainly caused by the following three phenomena:

1) The change in the refractive indices of the optical glasses from which the lenses are made.
2) The change in the radii and thicknesses of the lenses.
3) The change in the air-spaces between different lens groups.

The main effect of these changes is that it changes the power of the lenses and thereby causing defocussing. A secondary effect is the change in the aberrations (such as the Seidel aberrations). This will, to a lesser extent, also contribute to the degradation in performance as a function of temperature.

The calculation of the defocussing of an optical system due to temperature changes are presented below:

2.2.2 FOCUS SHIFTS DUE TO TEMPERATURE CHANGES.

The defocussing due to the expansion of the mounting material is calculated by the following well known formula:

(2.9) $dL = L_o \alpha_m dt$

where L_o is the length of the mechanical mount separating the lenses

dL is the change in L_o due to a temperature change of dt

α_m is the linear expansion coefficient of the mounting material

The defocussing caused by a change in power of the lenses due to changes in temperature requires special consideration:

The power of a thin lens suspended in air is given by the following equation:

(2.10) $K = (n-n')[c_1 - c_2]$

where n is the absolute refractive index of the lens material

n' is the refractive index of air

The change in power with temperature is given by:

(2.11) $$dK = (n - n')[c_1 - c_2]\,dt$$

$$= K\left[\frac{dn/dt - dn'/dt}{n - n'} - \alpha_g\right]dt$$

where α_g is the linear thermal expansion coefficient of the lens material.

The change in effective focal length f will thus be given by:

(2.12) $$df = 1/K\,dt$$

$$= f\left[\frac{dn/dt - dn'/dt}{n - n'} - \alpha_g\right]dt$$

$$= f\,\alpha_f\,dt$$

where α_f is the opto-thermal expansion coefficient of the lens material.

This quantity, α_f [8] is independent of the structural form

of the lens and is only a function of the properties of the glass. This coefficient can be considered to be similar to the known linear thermal expansion coefficient in that it gives the change in effective focal length of a thin lens with a change in temperature. The opto-thermal expansion coefficient, although temperature dependent, is fairly constant between -20 and +60 degrees celsius. For the purposes of first order design the opto-thermal expansion coefficient was assumed to be constant.

According to the definition of a thin lens (refer to 2.1.6), the effective and back focal lengths of thin lenses are equal. The opto-thermal expansion coefficient will thus also predict the change in back focal length of a thin lens. The aim during athermalization is to chose optical glasses and mounting materials such that the change in back focal length equals the expansion of the mounting materials, thereby eliminating defocus

A table of all the αf values for the Schott glasses of which the relavent information were available is given in decending order of αf values, in appendix A.

2.3 THEORY OF A Nd-Yag LASER.

The beam expander will transmit the radiation emitted by a Nd-Yag laser which has a crossed Porro prism resonator.

Since the laser and the beam expander is coherently coupled a fairly accurate model of the laser was required to be used during the design and especially during the evaluation of the laser/beam expander combination. This model will now briefly be presented:

2.3.1 SPECTRAL PROPERTIES OF THE LASER.

A NdYag laser emits radiation at a wavelength of 1064nm with a spectral bandwidth of only 0,4nm[10]. The dispersion caused by this spread in wavelength in normal optical glass is negligible. The radiation can therefore be treated as being monochromatic and no provision for the correction of chromatic aberration is thus required.

2.3.2 ILLUMINATION IN THE PUPIL OF THE LASER.

A crossed Porro prism resonator only supports the TEM01* mode[9]. The theoretical illumination in the pupil of a laser in the TEM01* mode is given[11] by the following:

$$I(r)=I_0(r/w)^2\exp(-2[r/w]^2) \qquad (2.14)$$

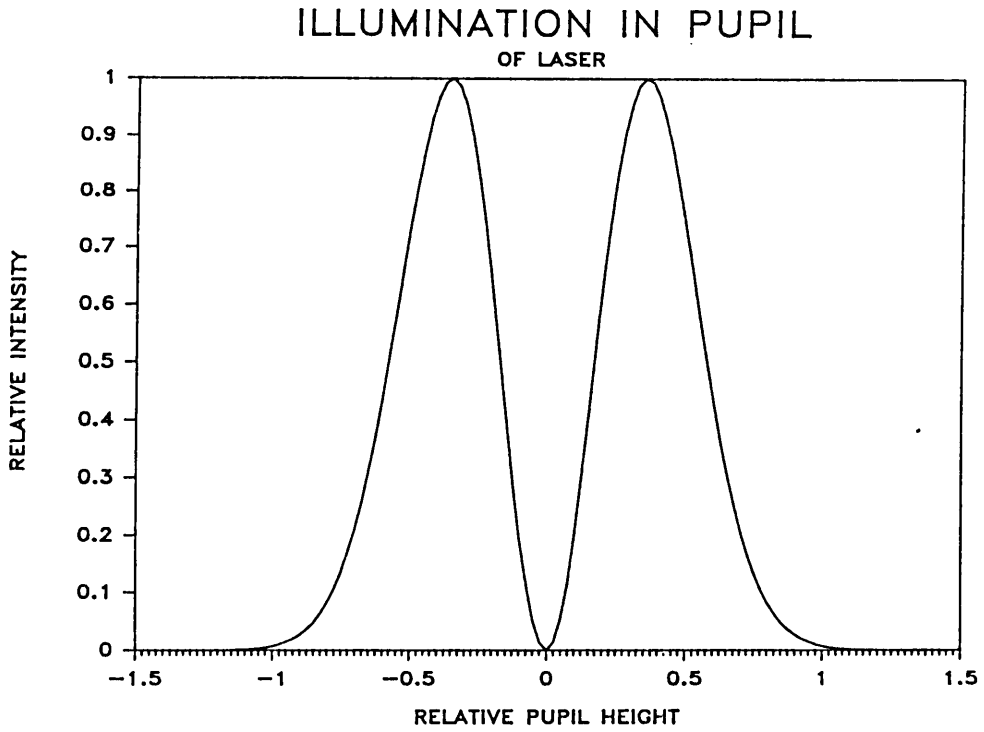

FIG 2.2 Illumination in the pupil of the laser

2.3.3 FAR-FIELD RADIATION PATTERN OF THE LASER.

The divergence of a laser is directly related to the far-field radiation pattern of the laser.

The general shape of the illumination pattern in the pupil of the laser is found to be preserved in the far-field radiation pattern[11]. Although neither Koechner nor Nortier provided any explicit formulae for the expected far-field pattern, graphs of measured values were given[9][11]. These graphs were approximated by the

following expression:

(2.15) $$I(\theta)=I_0(\exp[-8<(\theta-v)/v>^2] + \exp[-8<(\theta+v)/v>^2])$$

where θ is the field angle in mrad

v is the semi-divergence of the laser.

Eq. 2.15 was used to generate weigths for different field angles which were used to model the far-field radiation pattern of the laser.

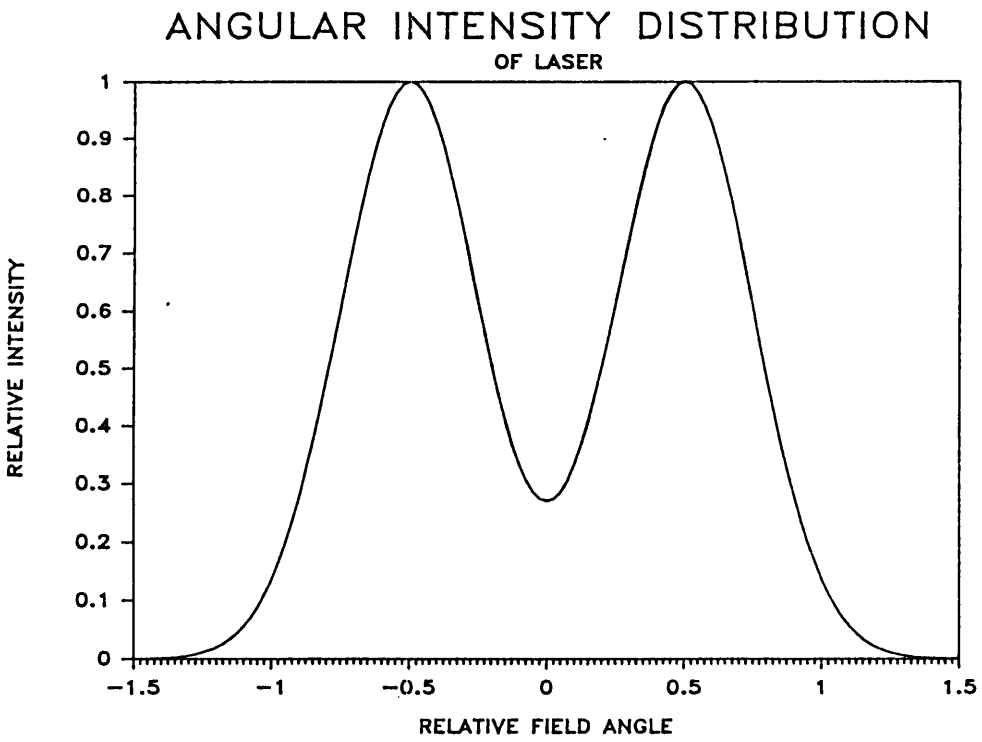

FIG 2.3 Far-field radiation pattern.

A graph of the far-field radiation pattern is given in fig 2.3

This radiation pattern will approximately be reproduced by the beam expander scaled by the magnification of the beam expander. Since the relative illumination in the centre of the radiation pattern is 0.27, it was expected that the illumination in the centre of the radiation pattern of the complete system will also be relatively low unless special precautions were taken to make the radiation pattern more uniform.

Eq. 2.14 and 2.15 was found to be sufficient to model the laser.

CHAPTER 3

3 THE DESIGN SPECIFICATIONS.

In this chapter the user requirements for the beam expander are translated into optical design specifications.

3.1 USER REQUIREMENTS

The optical and mechanical requirements which were received as an input to the design of the beam expander are discussed below. These requirements were not questioned although the implications thereof are highlighted.

3.1.1 OPTICAL REQUIREMENTS

THE SOURCE OF RADIATION

The beam expander shall be illuminated by a Nd-Yag laser with a crossed Porro prism resonator. The beam waist diameter of the laser is less than 7mm. The maximum divergence of this laser, defined as the angle subtended by two points opposite sides of the axis where the intensity

drops to e^{-2} of the peak intensity, is less than 1.9mrad.

DIVERGENCE REQUIREMENT

The divergence of the system shall be less than 0.3mrad at all temperatures between -20 and 60°C. Ninety percent of the energy emitted by the laser shall be transmitted into an angle of 0,3mrad.

3.1.2 MECHANICAL REQUIREMENTS.

TOTAL LENGTH REQUIREMENT

The total length of the beam expander, measured from the vertices of the first to the last optical surface shall be less than 120mm.

EXIT PUPIL DIAMETER

The maximum diameter of the exit pupil shall be 50mm.

These requirements are translated into design specifications relevant to the optical designer:

3.2 DESIGN SPECIFICATIONS

The magnification, optical performance specification and focal lengths were extracted from the user requirements as follows:

3.2.1 MAGNIFICATION SPECIFICATION

The theoretical divergence D of the complete system, assuming a perfect optical system is given by:

(3.1) $D >= d\ M$ or $M <= D/d$

where d is the divergence of the laser and
M is the magnification of the beam expander

The maximum magnification the beam expander can have, is M = 0.158. This boundary is depicted graphically at point A of fig.3.1.

The mechanical requirement that the exit pupil diameter shall be less or equal to 50mm, using a 7mm laser beam puts a lower bound to the magnification of the beam expander.

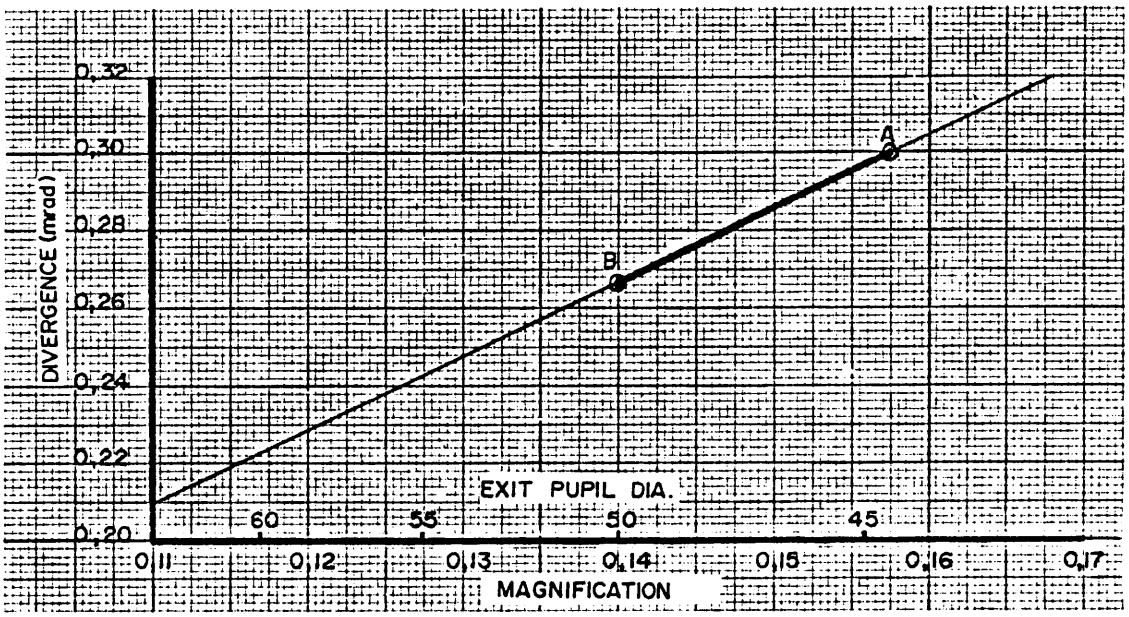

Fig. 3.1 Divergence versus magnification assuming a laser divergence of 1.9mrad

The exit pupil diameter, d_o, is given by the following equation:

(3.2) $d_o = d_i / M$ or $M = d_i / d_o$

where d_i is the diameter of the laser beam

The minimum magnification the beam expander can have is M = 0.14. This boundry is depicted graphically at point B of fig 3.1.

Now that the boundaries for the magnification are determined, a choice of a specific magnification has to be

made:

A magnification of 0.158 (point A in fig.3.1) is only achievable with an optical system which has no aberration. In practice the magnification has to be reduced to allow for the additional divergence caused by aberrations, manufacturing imperfections and diffraction. The smaller the magnification, the larger the aberrations etc. of the system can be.

The lower limit to the magnification is 0,14 times. A magnification of 1/7times (0.1429) was adopted for the first order design.

3.2.2 OPTICAL PERFORMANCE SPECIFICATION.

The total divergence of the system can be decomposed into the "intrinsic" divergence (due to the laser divergence and the magnification of the beam expander), and the divergence due to diffraction, aberrations, manufacturing tolerances, temperature changes etc.

A magnification of 1/7 times and a laser divergence of 1.9mrad yield an "intrinsic" divergence D, of 0,271mrad which is 0,029mrad less than the allowable maximum divergence. The divergence due to aberrations, diffraction

effects, manufacturing tolerances and temperature effects must thus be less than 0,029mrad. For the purposes of first order design the 0.029mrad was divided between the different contributers to the divergence. A realistic, but somewhat arbitrary error distribution is given below:

ERROR BUDGET

aberrations and diffraction:	70%	or	0,0200mrad
manufacturing tolerances:	15%	or	0,0045mrad
temperature effects:	15%	or	0,0045mrad

The allowable divergence due to temperature effects is small enough to ensure that the total divergence is insensitive to temperature changes, since it amounts to only 1.5% of the total divergence.

The 15% divergence due to manufacturing tolerances is 21% of the allowable divergence due to aberrations. Such a design will have relatively large manufacturing tolerances and would be relatively inexpensive to manufacture.

Finally, the 70% error budget on aberrations determines the complexity of the optical system.

3.2.3 FOCAL LENGTH CALCULATIONS.

The magnification of the beam expander is chosen to be 1/7 times. This choice implies a ratio of 1:7 between the focal lengths of the two lens groups f_1 and f_2 (refer to fig.3.2), thus:

$$|f_1/f_2| = 1/7 \tag{3.3}$$

The total length of the beam expander has to be less than 120mm. Thus, for a thin lens approximation:

$$f_1 + f_2 = 120\text{mm} \tag{3.4}$$

The following two solutions satisfy eq. 3.3 and 3.4 simultaneously

$f_1 = 15\text{mm}$ and $f_2 = 105\text{mm}$

or

$f_1 = -20\text{mm}$ and $f_2 = 140\text{mm}$

The first solution provides the first order configuration for an astronomical telescope, which will not be considered in this thesis. The F-numbers of the two lenses in this configuration would be F/2.1.

The second solution provides the first order configuration for a Galilean telescope. In this case the F-numbers are only F/2.9, which is advantageous since higher order aberrations decreases as F-number increases.

After carefully studying the pros and cons of the two telescope types the Galilean solution was chosen. A schematic of this telescope is shown in figure 3.2.

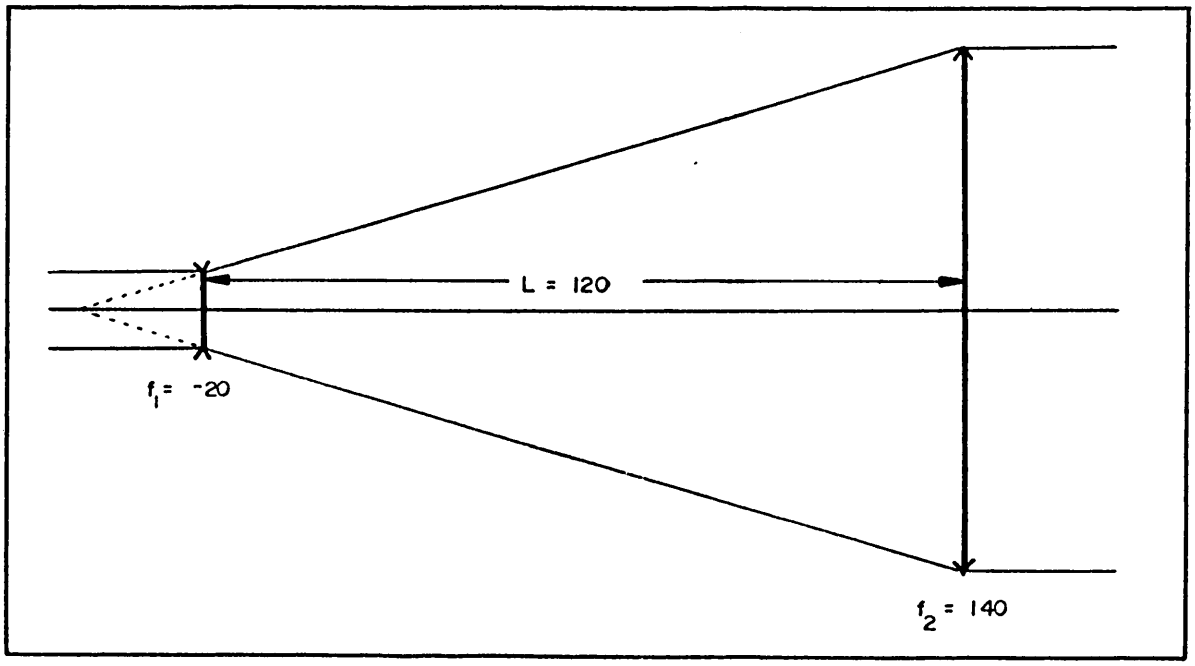

FIGURE 3.2 Schematic of the Galilean telescope

These focal lengths were used as a guideline for both the two and three lens beam expander designs which are presented in the following chapters.

CHAPTER 4

4 CONCEPTUAL DESIGNS.

The conceptual design of a TWO lens beam expander will be discussed in this chapter. Although the performance of this design proved to be insufficient in the end, the design will nevertheless be presented here, since it is useful for less demanding applications. A more complex, high performance design is presented in chapter 5.

4.1 TWO LENS BEAM EXPANDER

The design of the two lens beam expander consists of two parts. Firstly an athermal condition was generated and met and secondly the optical performance (aberrations) were controlled.

4.1.1 ATHERMALIZATION CONDITION.

A Galilean telescope will be athermal if the focal points of the two lens groups remain coincident over the desired temperature range. It is assumed that the temperature is at all times uniformly distributed throughout the optical system.

The changes in focal lengths of the two thin lenses with regard to a change in temperature are:

(4.1) $d(f_1) = \alpha_1 f_1 dt$

(4.2) $d(f_2) = \alpha_2 f_2 dt$

where α_1 denotes the αf value (Opto-thermal expansion coefficient) of lens no. 1 etc.

The change in distance l between the two lenses as a function of temperature (refer to fig. 3.2) is:

(4.3) $dl = l \alpha_m dt = (f_1 + f_2) \alpha_m dt$

where α_m is the linear thermal expansion coefficient of the material separating the two lenses.

The focal points of the two lens groups will stay coincident if the change in back focal lengths due to temperature changes is equal to the expansion of the mounting material, thus if:

(4.4) $d(f_1) + d(f_2) = dl$

But:

(4.5) $f_1 = M f_2$

where M is the magnification of the telescope.

Substituting 4.1, 4.2 and 4.3 into 4.4 yields:

(4.6) $\alpha_1 f_1 dt + \alpha_2 f_2 dt - (f_1 - f_2) \alpha_m dt = 0$

Substituting 4.5 into 4.6 yields:

(4.7) $\alpha_2 - M \alpha_1 = (1 - M) \alpha_m$

The aim is thus to design a system which would satisfy eq. 4.7. As a first attempt aluminium (Al) was chosen as a mounting material. The linear thermal expansion coefficient of Al is α_m = 23.6E-6 $^{\circ}C^{-1}$. If the two lenses are made from identical optical glass , then, by using eq 4.7:

(4.8) $\alpha_f = \alpha_m$ = 23,6E-6$^{\circ}C^{-1}$

The optical glass, with an opto-thermal expansion coefficient α_f closest to 23,6E-6$^{\circ}C^{-1}$ is the Schott glass LGSK2 with α_f = 19,1E-6$^{\circ}C^{-1}$. (See appendix A) By substituting this value into equation 4.6 the resultant defocussing D due to a temperature change will be:

(4.9) D = 120x19,1E-6 dt - 120x23,6E-6 dt = -.00054 dt

At a temperature of 50°C the defocus D equals -0,016mm. The maximum divergence of the beam expander due to this defocus is:

(4.10) Divergence = $h/f_1 - h/(f_1 + D)$

$= 24.5/140 - 24.5/(140-0.016)$

$= -0.020$mrad

This value is larger than the anticipated error budget for thermal effects in section 3.2.2.

4.1.2 THIRD ORDER ABERRATION CORRECTION.

In this section the third order spherical aberration of the two lenses are minimized and the resultant aberrations are calculated.

Assume the following first order layout. Let h_1 in fig 4.1, which is equal to 3.5mm, be the radius of the laser beam, and thus the height at which the marginal ray strikes the first lens. Let $K_1 = -1/20$ be the power of the first lens. [The power of a thin lens suspended in air is equal to the reciprocal of the effective focal length of the lens]. Let $h_2 = 24.5$mm be the height at which the marginal ray strikes the second lens, which has a power of $K_2 = 1/140$. Let l =

120mm be the distance between the two lenses. The refractive index of the two lenses, made from LGSK2, is n = 1.575239.

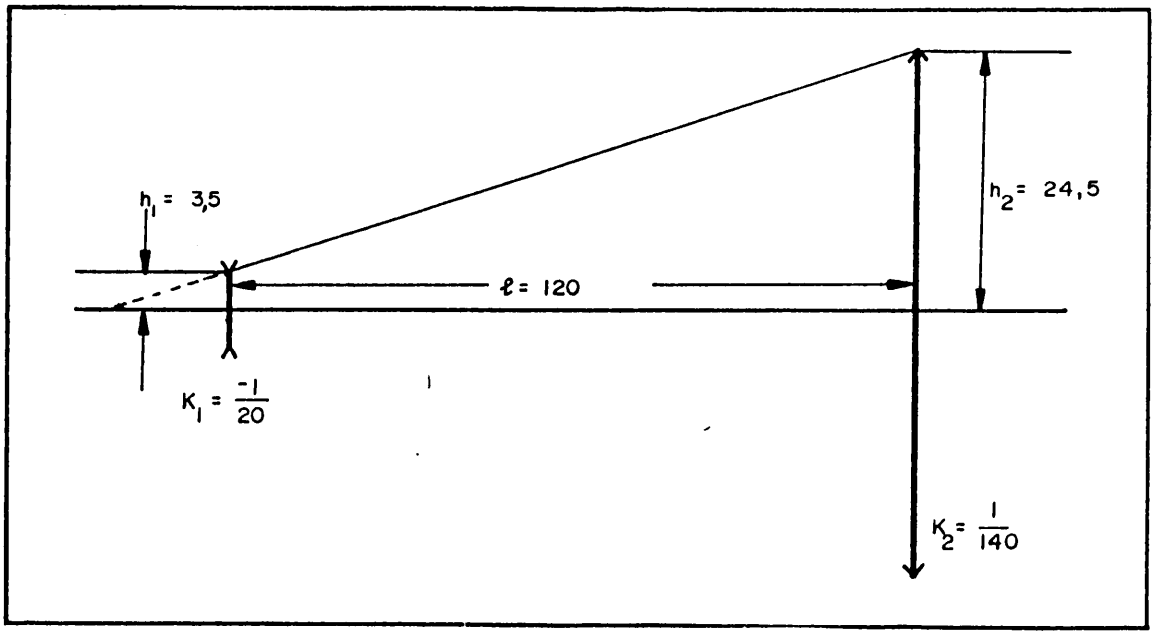

Fig. 4.1 Thin lens layout

In order to calculate S_1 the conjugate variable for each lens is required. From eq 2.6 the conjugate variables C_1 and C_2 of the first and second lenses are:

(4.11) $C_1 = -h_1 K_1$

$= 0.1750$

(4.12) $C_2 = h_2 K_2$

$= 0.1750$

$= C_1$

The third order spherical aberration S_1, for each thin lens, given by eq 2.7, has an extreme value where:

(4.13) $B = -2C(n+1)/(2+n)$

For a thin lens with one infinite conjugate, thus $C^2 = (hK)^2$, the extreme value for S_1 reduces to:

(4.14) $S_1(ex) = (h^4K^3/4)\,[n/(n-1)]^2 + n/(n+2)\,)$

The maximum S_1 of the first lens, S_{11}, and the minimum S_1 for the second lenses, S_{12} are:

(4.15) $S_{11}(max) = -.0331 \quad (B_1 = -0.2521)$

(4.16) $S_{12}(min) = 0.2317 \quad (B_1 = -0.2521)$

The only way in which the total S_1 can be reduced is to decrease the value of S_{11} so as to exactly cancel S_{12}. The new target for S_{11} is therefore:

(4.17) $S_{11} = -.2317$

By substituting eq 4.17 and 4.11 into eq 2.7 and solving for B_1 the following two solutions are found:

(4.18) B_1 = 0.50384 or -1.0080

From these values of B_1 and B_2 (eq.4.16), via eq 2.5 and 2.10 two sets of radii (one set for each value of B_1) were calculated.

The two resultant third order designs are given below:

First solution (B_1 = 0.50384):

Radii	Material	Thickness
35,0675	LGSK2	0,0
8,6627	AIR	120
940,1133	LGSK2	0,0
-88,0759	AIR	---

Second solution (B_1 = -1.0081):

Radii	Material	Thickness
-5,3343	LGSK2	0,0
-9,9457	AIR	120
940,1133	LGSK2	0,0
-88,0759	AIR	---

The angular ray aberrations of both solutions are shown in fig.4.2

Although both of the above solutions have zero third order spherical aberration, the higher order aberrations of the second solution exceed that of the first solution. This is to be expected since the radii in solution II are

considerably shorter.

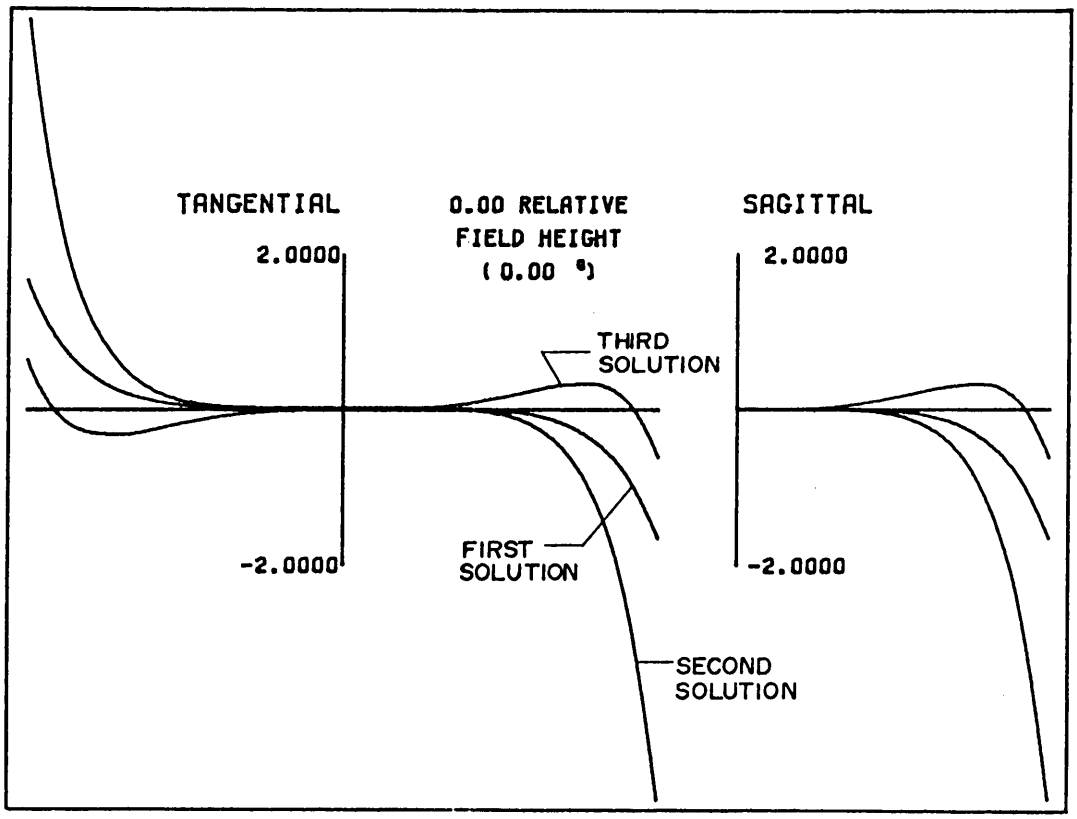

Fig. 4.2 Angular ray aberrations in mrad

The first solution, which is therefore more promising as far as aberration correction is concerned, has an angular ray aberration, ARA(1.0) of -1.660mrad at a relative aperture of 1.0. Thus:

$$ARA(1.0) = -1.660 \text{ mrad}$$

The finite angular ray aberration of a lens at x relative aperture, ARA(x), can be decomposed into the third order angular ray aberation, TARA(x) and the higher order angular ray aberration HARA(x) as follows:

(4.21) $ARA(x) = TARA(x) + HARA(x)$

The third order angular ray aberrations can be linked to the third order spherical aberration, S_I, by:

(4.22) $TARA(x) = S_I x^3/(2nh)$

where h is the radius of the exit pupil
n is the refractive index of image space

Since the TARA(1.0) of the present solution is zero it implies (according to eq 4.21) that:

(4.23) $ARA(1.0) = HARA(1.0) = 1.660\text{mrad}$

Since the TARA can be controlled the ARA was reduced by introducing TARA such as to cancel the HARA of the design. The new target for the TARA(1.0) was chosen to be 1.660 instead of zero. A target of 1.660 implies (according to eq.4.22) an S_I of -0.0813. The S_I for the complete system was then increased by adding -0.0813 to the target for S_I thus:

$S_{1\,1} = -0.2317 + -0.0813 = -0.3130.$

This target rendered bendings of $B_1 = 0.6453$ or -1.1493. The first value for B_1 gave the least higher order aberrations and was used. The resultant solution is:

Third solution ($B_1 = 0.6453$):

Radii	Material	Thickness
20,5217	LGSK2	0,0
7,3720	AIR	120
940,1133	LGSK2	0,0
-88,0759	AIR	---

The angular ray aberrations, ARA, of this third solution are also presented in fig 4.2. The ARA(1.0) equales -0.627 as compared to -1.660 of the first solution.

Further iterations to optimize the balance between the third and higher order aberration were done and the ARA of the resultant design is given in fig 4.3.

Sufficiently good performance could still not be achieved. The expected divergence due to aberrations of the final design (which is approximated by the RMS of the ARA) is about 0.2mrad.

The divergence due to aberrations and temperature effects is

much larger than allowed for in the error budget and both had to be improved.

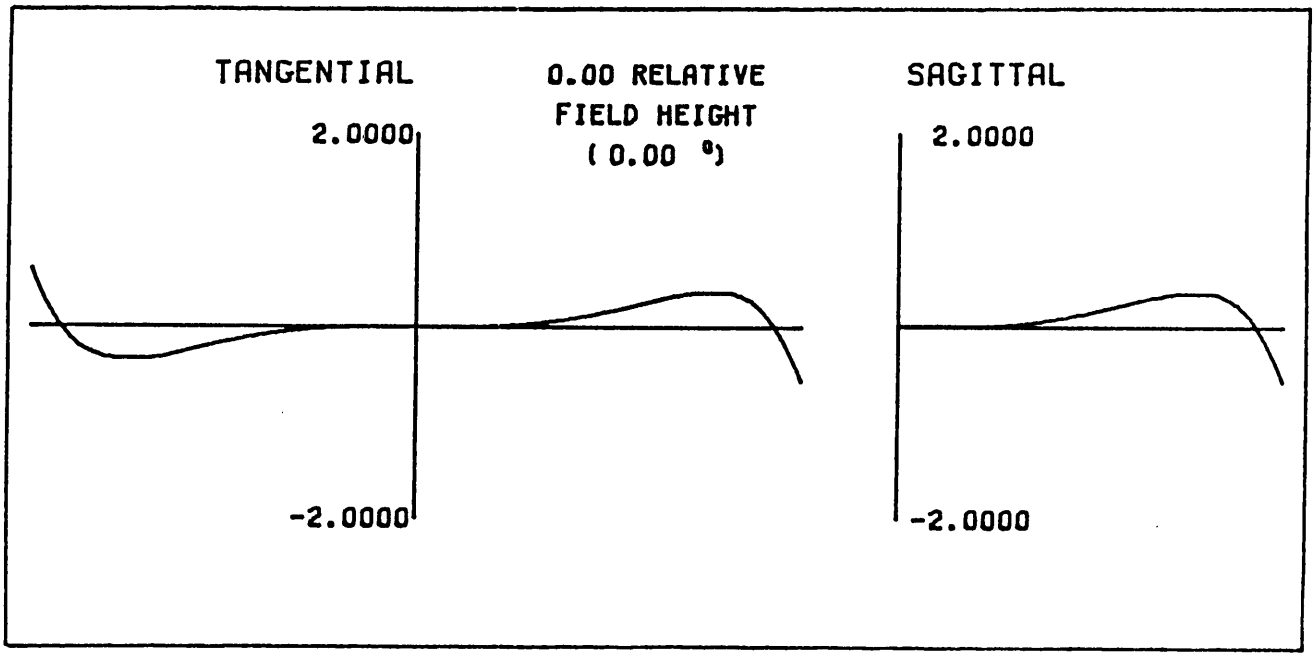

Fig. 4.3 Angular ray aberration of the optimized thin lens in mrad

4.2 IMPROVED TWO LENS BEAM EXPANDER DESIGN.

The aim was to maintain the basic structure of the design but to reduce the divergence.

The athermalization correction was improved by a better choice of

glasses and mounting materials, whilst the aberration correction was improved by choosing glasses with higher refractive indices. This approach is presented below:

4.2.1 IMPROVED ATHERMALIZATION:

After inspection of eq 4.7 it was clear that α_1 had to be as large as possible and α_2 as small as possible in order to meet the α_m of available mounting materials.

The two most extreme glasses (as far as opto-thermal expansion coefficient are concerned) having high (larger than 1.75) refractive indices as well as good physical properties are LASF9 and SF11, with opto-thermal expansion coefficients of 3.1E-6 and -3.2E-6°C^{-1} respectively. With this glass choice a mounting material with an α_m = 4.35E-6°C^{-1} will give perfect athermalization. The mounting material having an α_m closest to 4.35E-6°C^{-1} is nickel (Ni), with an α_m = 3.7E-6°C^{-1}. Substituting this value back into eq 4.7 and making α_2 a variable, gives α_2 = 1.5E-6°C^{-1}. A good fit for this value is K50 with an α_2 of 1.4E-6°C^{-1}. This slight mismatch introduces a divergence of 0.002mrad, which is within the error budget generated in section 3.2.2

4.2.2 IMPROVED ABERRATION CORRECTION

Different glass types were used and tried in order to find a

solution with better aberration correction. The best correction was found by designing f_1 with a low refractive index glass and f_2 with a high refractive index glass. The glass choice of K50 and LASF9 thus satisfies both the new athermalization as well as the aberration correction requirement. The aberration correction method was similar to that of the previous design . The resultant angular ray aberrations are shown in fig 4.4.

As is evident from this figure, the new design is superior to the previous attempt. Unfortunately, however the aberrationms are still by a factor two too large.

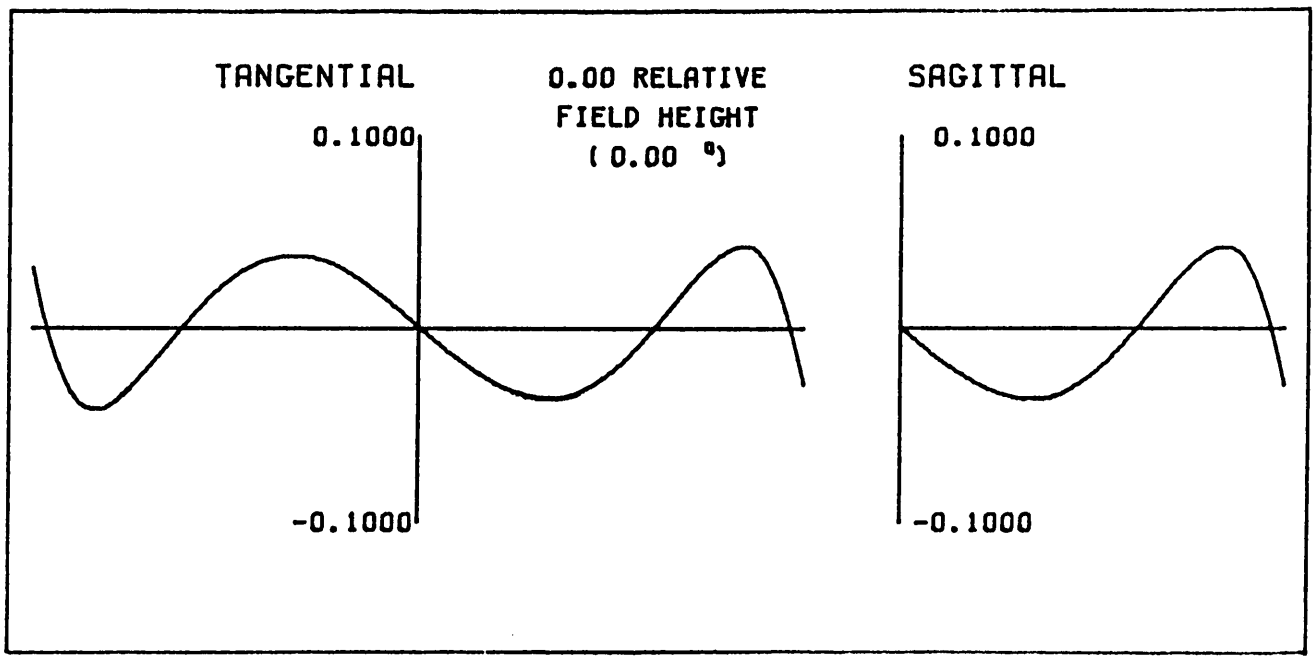

Fig. 4.4 Angular ray aberrations in mrad

4.2.3 SUMMARY.

It was clear that the required performance could not be obtained with the present two lens system. Apart from the fact that a satisfactory state of correction could not be achieved, the athermalization condition could also not be met precisely. The success in athermalization was dependent upon the spread in opto-thermal expansion coefficients of available processable optical glass and mounting materials. This implied that no "fine tuning" could be done if it was found that the thin lens athermalization (refer to 2.2.2) differed significantly from the real thick lens solutions.

A completely new approach was thus indicated, pointing into the direction of a somewhat more complex optical system. The design of such a system is presented in the next chapter.

5 CONCEPTUAL DESIGN OF THE THREE LENS BEAM EXPANDER.

The final approach which rendered sufficient performance uses the same basic construction as the previous designs except that the second lens, which was a singlet is now replaced by two lenses. This design required a completely new approach to athermalization as well as aberration correction.

Initially the mechanical specifications are satisfied by again generating a first order layout. Secondly, a thin lens athermalization technique is derived and applied to the first order design. The resultant thin lens design is then thickened to arrive at the final beam expander layout.

5.1 FIRST ORDER CALCULATIONS.

The thin lens layout for the three lens system is shown in fig 5.1

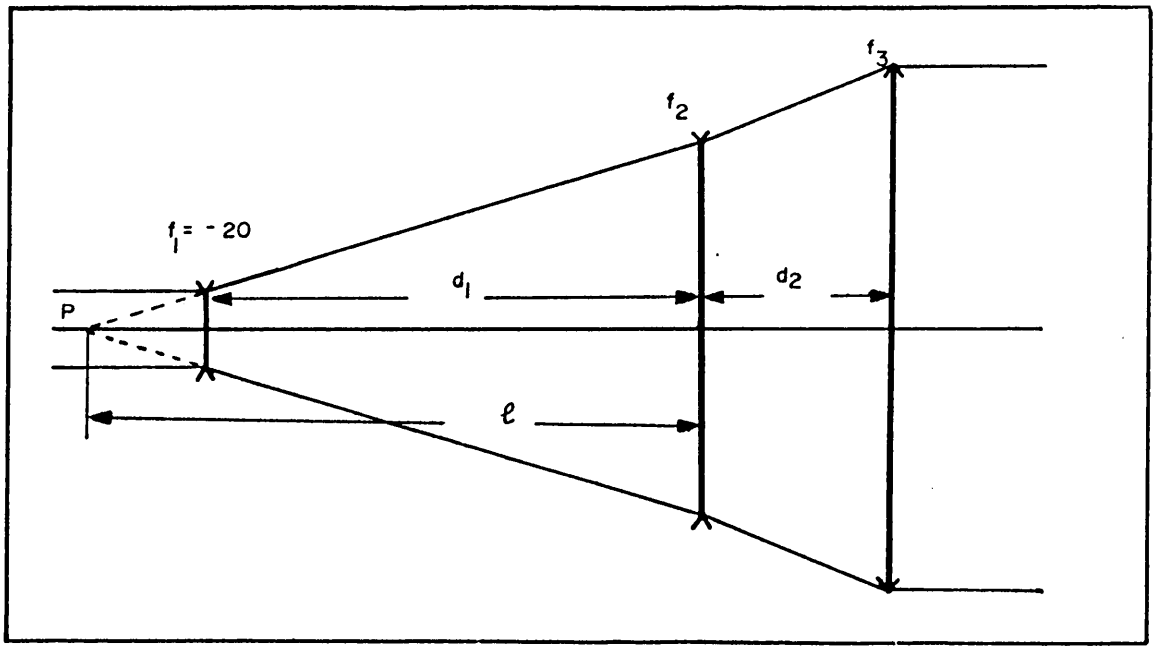

Fig 5.1 Thin lens layout of the three lens system

The design parameters which were generated in section 3.2 are summarised below:

Magnification:	1/7
Entrance pupil diameter:	7mm
EFL of f_1	-20mm
EFL of (f_2 + f_3)	140mm
Overall length	<120mm

Four equations are presented which controlles the relationship between the various variables:

5.1.1 OVERALL LENGTH REQUIREMENT

The FIRST relationship is the relationship between d_1 and d_2 (refer to fig.5.1). In order to keep the overall length less than 120mm:

$$d_1 + d_2 <= 120mm$$

Assume that:

(5.1) $$d_1 + d_2 = 110mm$$

A value of 110mm instead of 120mm is used to accommodate a possible lengthening due to lens thickening (bear in mind that this is a thin lens approach).

5.1.2 MAGNIFICATION REQUIREMENT

The SECOND condition to be controlled is the magnification of the beam expander. The effective focal length of the first lens f_1 has to be -1/M times that of the effective focal length of the second and third lens combination. Thus:

(5.2) $$-M/f_1 = 1/f_2 + 1/f_3 - d_2/(f_2 f_3)$$

5.1.3 AFOCAL REQUIREMENT

The THIRD condition to be controlled is that the beam expander has to be afocal. This implies that the focal points of the first lens and the second lens group had to coincide (P in fig 5.1). This is true if $d_1 - f_1$ is equal to the front focal length of the second lens group. Thus:

$$(d_1 - f_1)^{-1} = f_2^{-1} + (f_3 - d_2)^{-1} \tag{5.3}$$

5.2 ATHERMALIZATION OF THE THIN LENS DESIGN.

The FOURTH and last condition to control is that the focal points have to stay coincident at all temperatures. This implies that l (refer to fig 5.1) as seen from f_1, and l as seen from the f_2/f_3 combination have to stay equal at all temperatures.

The value l as seen from f_1 is:

$l = d_1 - f_1$ thus:

$$dl = (d_1 \alpha_m - f_1 \alpha_1)dt \tag{5.4}$$

The value of l as seen from the f_2/f_3 combination is:

$l = (1/f_2 + 1/(f_3 - d_2))^{-1}$ thus:

$$(5.5) \qquad dl = l^2 \left[\frac{\alpha_2}{f_2} + \frac{f_3\alpha_3 - \alpha_m d_2}{(f_3 - d_2)^2} \right] dt$$

For the beam expander to be athermal the value dl in eq.5.4 and 5.5 have to be equal, thus:

$$(5.6) \qquad \frac{d_1\alpha_m - f_1\alpha_1}{(d_1 - f_1)^2} = \frac{\alpha_2}{f_2} + \frac{f_3\alpha_3 - d_2\alpha_m}{(f_3 - d_2)^2}$$

If equations 5.1, 5.2, 5.3 and 5.6 are solved simultaneously, the only remaining requirement to satisfy is the optical performance requirement. This will be presented in section 5.4.

5.3 FIRST ORDER LAYOUT.

Assume that $f_1 = -20$ and $M = 1/7$. Solving equations 5.1, 5.2, 5.3 and 5.6 simultaneously yields:

$$(5.7) \qquad d_2 = \frac{1300\alpha_2 - 1400\alpha_3 + 100\alpha_m}{-20\alpha_1 - 10\alpha_2 + 140\alpha_3 - 130\alpha_m}$$

The first order layout as well as the athermalization requirement is thus solved analytically, and the result is not dependant on the spread in opto-thermal or linear expansion coefficients. If the thin lens athermalization differs slightly from the thick lens solution the value for d_2 could be "tuned" to perfect the athermalization. (The two lens athermalization condition

[eq.4.7] required a discreet jump to another glass choice.)

From a practical point of view the value of d_2 has to be positive and also less than 110mm. This criterion limited the choice of mounting materials. For example, by choosing aliminium (Al) as a mounting material and using average optical glasses, the value for d_2 was too small. To find realistic values for d_2, α_1 and α_2 hav to be as small (negative) as possible and α_3 has to be as large as possible. The two most extreme glasses which still have high refractive indices and sufficient chemical and environmental properties are SF11 and LAF22. LASF9 was not chosen being more expensive than LAF22. Substituting the opto-thermal expansion coefficient of these glasses and the linear expansion coefficient of Stainless steel (EN19) into eq.5.7 give:

(5.8) $d_2 = 18.18874$

The other variables are:

(5.9)
$$f_1 = -20.0000$$
$$f_2 = -203.3710$$
$$f_3 = 90.3348$$
$$d_1 = 91.8113$$

These first order parameters are accepted for the first order layout of the athermal laser beam expander. This ensures that the mechanical requirements as well as the athermal condition for

thin lenses are met. The only remaining requirement is the performance requirement and thus the correction of aberrations:

5.4 THIRD ORDER ABERRATION CORRECTION.

A schematic of the thin lens design is given in fig.5.2

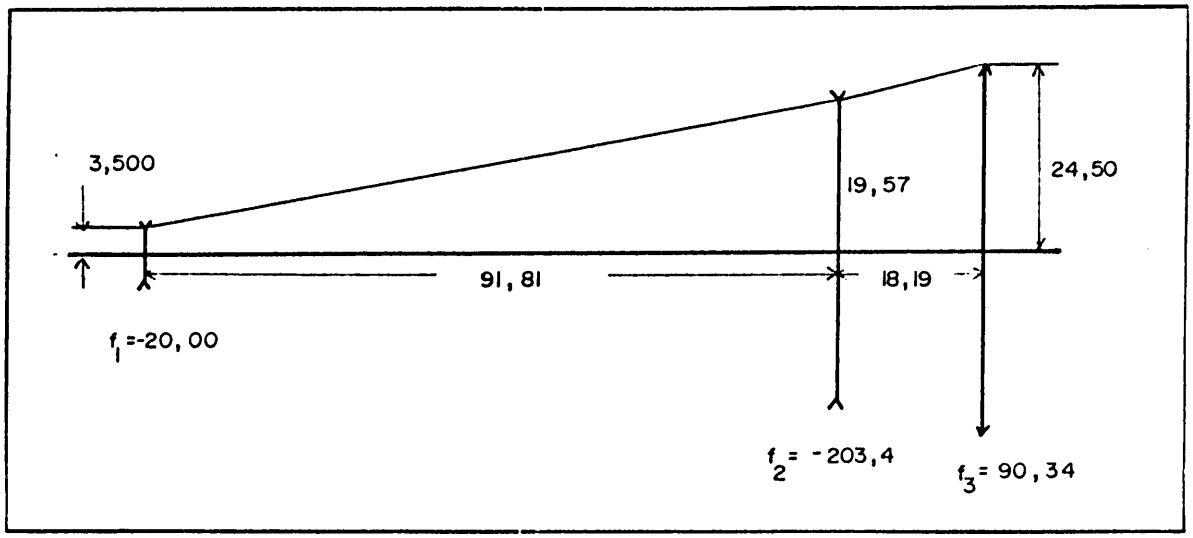

Fig 5.2 Layout of the thin lens design

As was pointed out previously the only third order aberration which needs to be controlled is spherical aberration, S_I. The aim is to generate the bending values for each lens which would make the total S_I zero:

The first step is to calculate the conjugate variables for each

lens. According to eq. 2.6 the conjugate variables are:

$$
\begin{aligned}
C_1 &= 0.0 + 3.5/20 &&= 0.175000 \\
C_3 &= 24.5/90.3348 + 0.0 &&= 0.217213 \\
C_2 &= C_1 + C_3 &&= 0.446213
\end{aligned}
\qquad (5.10)
$$

From thin lens theory the heights at which the marginal rays strike the lenses are:

$$
\begin{aligned}
h_1 &= 3.50000 \\
h_2 &= 19.56697 \\
h_3 &= 24.50000
\end{aligned}
\qquad (5.11)
$$

The extreme values for S_1 for each lens are then calculated with the aid of eq 4.14 and are presented in table 5.1

TABLE 5.1
Thin lens parameters of the thin lens design

lens no.	Ci	Bi	hi	efl	S_1(ex)
1	0.175000	-.2568	3.5000	-20.0000	-.023173
2	0.446213	-.6547	19.5670	-203.371	0.020223
3	0.217213	-.3981	24.5000	90.3348	0.598900
				(Total)	0.595950

The values for S_1(ex) in table 5.1 for lens 1 and 2 (both being of the negative power) are thus the LARGEST values the lenses can have while the value for lens 3 is the SMALLEST value S_1 can have. The total S_1 can thus only be reduced by decreasing the S_1 of lens 2.

The S_1 for lens 2, S_{12} is chosen such that the total S_1 equals zero, thus:

(5.12) $S_{12} = -(-.023173 + 0.598900)$

$= -.575873$

The corresponding bending, B_2 for lens 2 is:

(5.13) $B_2 = 0.114490$ or -1.423930

Both of these bendings were used to generate thin lens solutions. The optical system, as a consequence of the second value of B_2, produces twice the amount of higher order aberrations compared to the solution where the first value of B_2 is used. Lenses with bending values close to zero thus generated less higher order aberrations.

During the remaining design, bending values as close as possible to zero are used without neglecting the third order aberration correction requirements.

The absolute values of B_1 and B_3 (refer to table 5.1) were then reduced in an attempt to reduce the higher order aberrations. The value for B_1 was made zero and the value of B_3 was reduced to 2/3 of the original value. The value of B_2 was increased from 0.114490 to 0.14046 to keep the total S_1 equal to zero.

The new values for the bendings as well as the resultant S_I values are presented in table 5.2. Note that all the values are closer to zero.

TABLE 5.2
New bending and aberration values

lens no.	Bending (B)	Spherical aberration (S_I)
1	0.00000	-0.044779
2	0.14046	-0.616640
3	-0.26540	0.661419
	(total)	0.000000

Other bending values were also tried but the values presented in in table 5.2 were found to be the best compromise.

These values were used to generate the radii for the first thin lens design, via eq 2.5 and 2.10. The results are given in table 5.3

Obviously the third order spherical aberration S_I is very well corrected. The angular ray aberrations at 1.0 relative aperture is ARA(1.0) = 0.320mrad. The ARA(1.0) for an equivalent solution using the bendings given in table 5.1 is about twice as large.

TABLE5.3
Paraxial quantities of the thin lens design

Radius (R)	Thickness (t)	Angle of marginal ray (u)	Height of marginal ray (h)	Si surface contribution
-30,1730	0,0000	0,04988	3,5000	-,00134
30,1730	91,8113	0,17500	3,5000	-,04344
3032,06	0,0000	0,09698	19,5670	0,07713
146,020	18,1887	0,27121	19,5670	-,69376
533,687	0,0000	0,13436	24,5000	0,48006
-78,695	259,0E6	0,00000	24,5000	0,18136
			(total)	0,00001

The ARA(0.7) = 0.047mrad indicates that the remaining aberrations are mainly 5-th order spherical aberration.

5.5 THE THICK LENS DESIGN

The thin lens design presented above is a theoretical concept. Since manufacturable lenses must have thickness the thin lens design had to be converted to a thick lens design.

The theory of lens thickening will now be presented:

5.5.1 THEORY OF LENS THICKENING.

The aim during lens thickening is to keep the refraction at each surface of the thick design equal to that of the thin lens design. After thickening the aberration which may arise due to thickening would be corrected for, if required.

The ray deviation due to refraction of an optical system (in the paraxial region) is given by:

(5.14) $$u'n'-un = -h(n'-n)/R$$

where u and u' are the angles of the ray before and after refraction,
n and n' are the refractive indices of the media separated by the surface,
h is the height at which the ray strikes the surface,
R is the radius of the surface.

If the value of h/R is kept constant the refraction at the surface will also remain constant. The aim is thus to maintain the original value of h/R after thickening.

The values of u, h and R for each surface of the thin lens design are given in table 5.3

5.5.2 THICKENING OF THE FIRST LENS.

The first radius given in table 5.3 is maintained, and the thickness of the first lens is increased to 2.0mm. Due to this increase, the marginal ray intersects the second surface at a height h', given by:

(5.15) $h'_2 = h_2 + u_1 t_1$

where h_2 is the height at which the ray strikes the second surface of the thin lens,

h'_2 is the height at which the ray strikes the second surface of the thick lens,

u_1 is the angle of the ray inside the lens

t_1 is the thickness of the lens

To keep the refraction at surface 2 constant, the value of R_2 is changed to R'_2 such that:

(5.16) $h_2 / R_2 = h'_2 / R'_2$

where the primed values refer to values of the thick lens, thus:

(5.17) $R'_2 = R_2 (h_2 + u_1 t_1)/h_2$

$= 30.1730(3.5+.04988x2.0)/3.5$

$= 31.032920$

The new value for the air space following the lens t_2 is

given by:

(5.18) $t_2 = (h'_2 - h_2)/u_2$

,

where h_2 is the height at which the marginal ray, intersects the following surface,
u_2 is the angle of the ray following the second surface.

In the beam expander the thickness following surface 2 is equal to 91.241243.

The S_1 of this solution changed from zero to -0.00124, while the ARA(1.0) changed from 0.320 to 0.347mrad, which was a small enough change and did not require corrective action.

5.5.3 THICKENING OF THE THIRD LENS.

It is important to do the next thickening from the opposite side of the system: During thickening the heights at which the rays intersects the surfaces successively change which implies that the last ray height could end up completely different from the heights predicted by the thin lens design. This would change the exit pupil diameter of such a design. This effect is counteracted by increasing the thickness of the last lens from the opposite direction i.e. from surface 6.

Radius 6 is maintained and the thickness of the lens is increased to 9.0mm. The radius of surface 5 changed to 507.344 and the thickness of surface 4 to 13.7302.

The S_1 of the design changed to -0.0249. This is more than can be tolerated and is reduced by increasing the S_1 target of the second lens which is not yet thickened.

The S_1 target for the second lens, (S_{12}), is increased from -0.616640 (according to table 3.2.) to -0.5917 in an attempt to restore the total S_1 to zero.

This new S_{12} target implies a bending, B_2 = 0.124736 and radii equal to -13911.0 and 155.118. These values are substituted into the system and rendered a S_1 of zero and an ARA(1.0) of 0.338mrad. This is very close to the ARA(1.0) of the original thin lens design.

5.5.4 THICKENING OF THE SECOND LENS.

The radius of surface 3 is kept constant and the thickness of the second lens is increased to 3.5mm. The new radius of surface 4 is 157.903 and the thickness of surface 4 changes to 12.43510. The S_1 of the system changes to -0.011869 and the ARA(1.0) is 0.657mrad.

5.6 OPTIMIZATION OF THE REAL ABERRATIONS.

The finite angular ray aberrations of 0.657 at full aperture are reduced by adding some third order spherical aberration, S_I, to the system. The technique, previously discussed in section 4.1.2, is used to calculate the amount of S_I which will cancel the remaining real aberrations. According to eq 4.22 an S_I of 0.0322 will cancel the real aberrations at a relative aperture of 1.0. The S_I target for lens 2, S_{I2} is thus incremented by 0.0322. The new target for S_{I2}, is -0.5595 and renderes a bending B_2 of 0.10391. The resultant radii are -1658.41 and 169.045 respectively. The thicknessesHof surfaces 3 and 4 are also changed to their original values of 0.0 and 13.7303 respectively. The lens is then re-thickened similar to the previous procedure to a thickness of 3.5mm. The radius of surface 4 changed to 172.214 and the thickness of surface 4 to 12.3774.

The S_I for this design is 0.02058 and the ARA(1.0) and ARA(0.7) are equal to -0.197 and -0.1118 respectively. The relation between ARA(1.0) and ARA(0.7) is approximately linear which indicates that the finite aberrations can be reduced by defocussing the beam expander. An increase of -0.1278mm in the thickness of of the air space following surface 2 made the ARA(0.7) equal to zero. The resultant aberrations are presented in fig 5.3 (non-optimized).

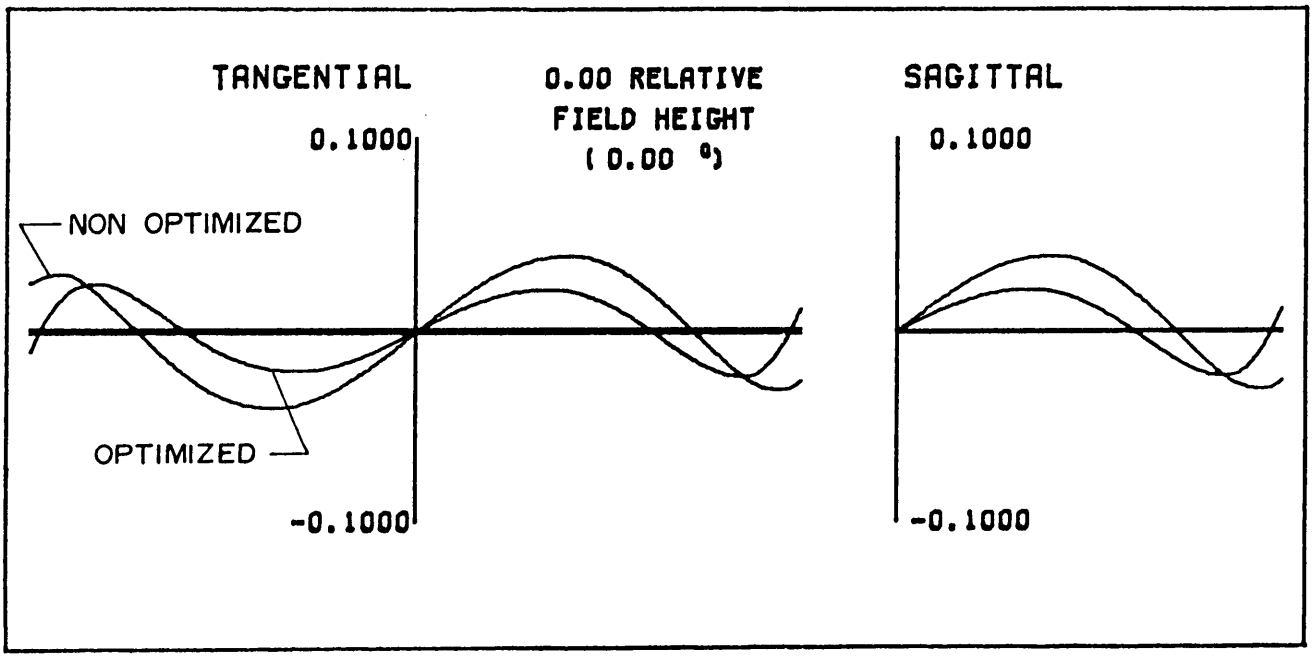

Fig. 5.3 Angular ray aberrations in mrad

From this graph it can be seen that the beam divergence can be reduced further by purposely deviating from the paraxial afocality constraint (thus by defocussing), and by tuning the third order aberration targets. This has the effect of compensating the higher order aberrations. An automatic computer program was used to optimize the balance between the defocussing and third order aberrations. The resultant angular ray aberrations of the computer optimized design are also given in fig.5.3. The constructional parameters of this final design are given in table 5.4, and the evaluation is presented in chapter

6.

TABLE 5.4
Constructional parameters of the design at 20°C

Radius	Thickness	Medium	Refractive index
-28,184	2,0000	SF11	1.754324
34,429	93,3607	AIR	1.000000
-860,98	3,5000	SF11	1.754324
170,31	11,5220	AIR	1.000000
473,115	9,0000	LAF22	1.759199
-77,203	-----	AIR	1.000000

CHAPTER 6

6 EVALUATION OF THE FINAL DESIGN.

In this chapter the evaluation of the final design will be presented. It will be shown that the design meets all requirements demanded in chapter 3.

6.1 EVALUATION OF THE FIELD AND TEMPERATURE DEPENDENCE OF THE DESIGN.

It will be recalled that the athermalization of the design was implemented by using the thin lens athermalization technique discussed in section 2.2. It will now be shown that this technique proved to be sufficiently accurate for the design of this beam expander.

The effects of temperature changes on the design were calculated in the following manner:

Changes of radii and thicknesses were simulated by using the well known linear thermal expansion equation, eq 2.9, while changes in refractive index were taken from the Schott optical glass catalogue. The changes of air spaces were calculated assuming

that the lenses were mounted in stainless steel (EN19) which has a linear thermal expansion coefficient of 11.1E-6°C⁻¹.

The resultant lens parameters at -20 and +60°C are given in table 6.1 and 6.2 respectively. A table for 20°C has already been presented in chapter 5 and will not be repeated here.

TABLE 6.1
BEAM EXPANDER AT -20°C.

Radius	Thickness	Medium	Refractive index
-28,17725	1,999521	SF11	1,754521
34,42076	93,316910	AIR	1,000312
-860,7739	3,499162	SF11	1,754521
170,2692	11,516448	AIR	1,000312
473,0208	8,997542	LAF22	1,759661
-77,18151	---	AIR	1,000312

TABLE 6.2
BEAM EXPANDER AT +60°C.

Radius	Thickness	Medium	Refractive index
-28,19101	2,000497	SF11	1,755117
34,43756	93,404509	AIR	1,000237
-861,1194	3,500870	SF11	1,755117
170,3523	11,527640	AIR	1,000237
473,2857	9,002582	LAF22	1,759729
-77,22475	---	AIR	1,000237

The angular ray aberrations of the beam expander at -20, 20 and 60°C on-axis and at a field angle of 1mrad are shown in figs 6.1 - 6.3.

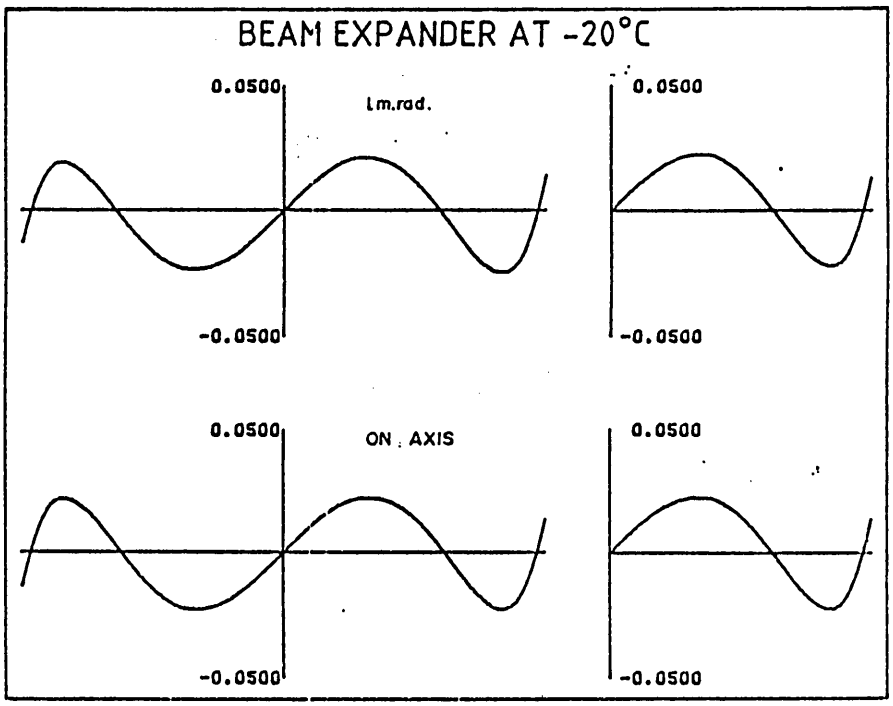

Fig 6.1 Angular ray aberrations in mrad

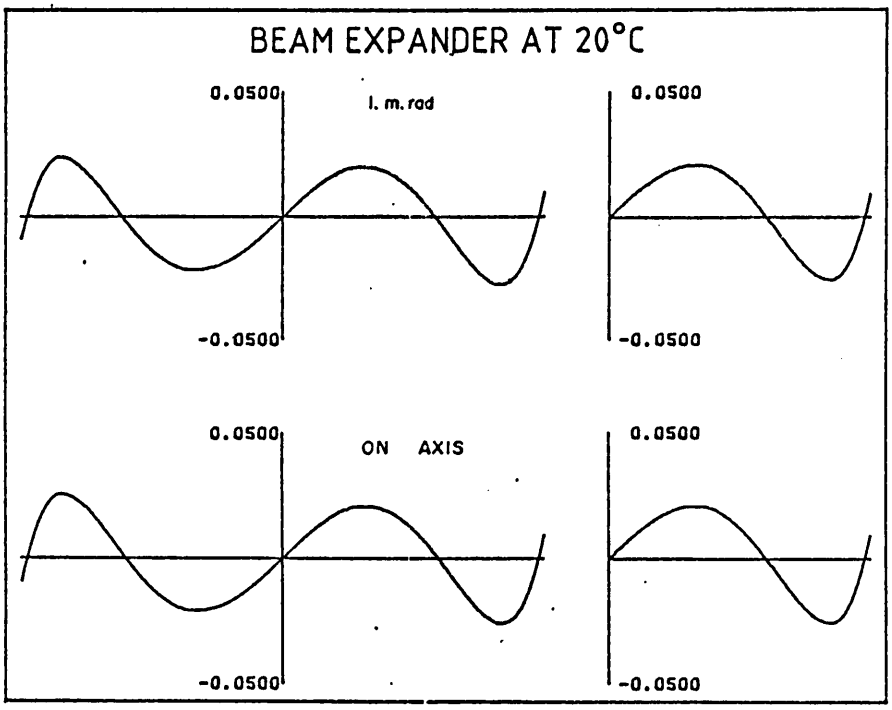

Fig 6.2 Angular ray aberrations in mrad

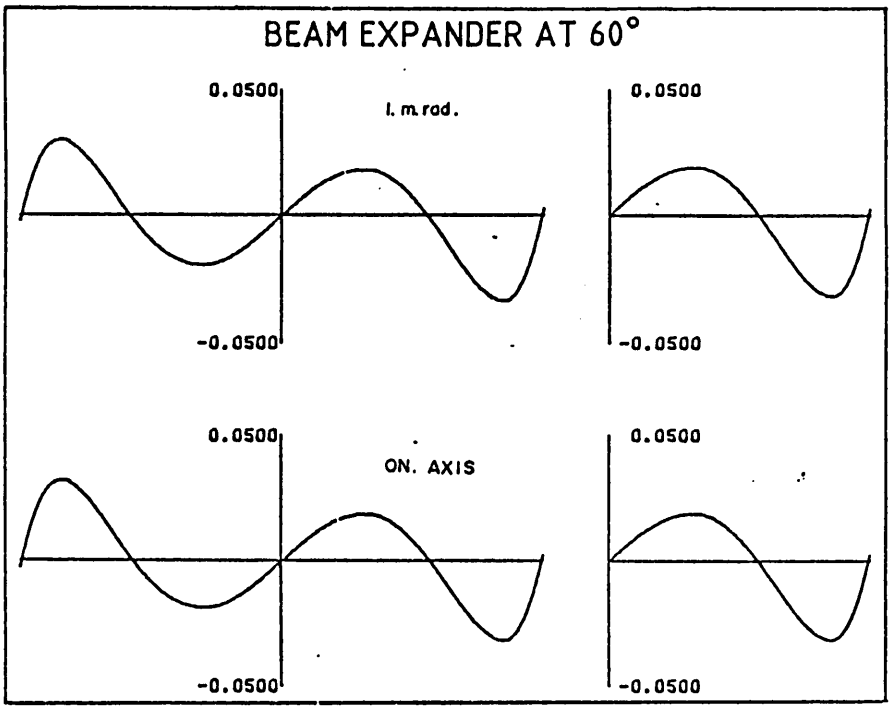

Fig 6.3 Angular ray aberrations in mrad

These graphs show that the divergence is minimally effected by a change in temperature. The maximum change in divergence due to extreme temperature variations at full aperture amounts to only 0,0048mrad. Since most of the energy from the laser passes through the beam expander at relative aperture heights of between 0,3 and 0,7 the expected significant divergence due to temperature variations will be less than 0,0034. This is equivalent to the divergence at a relative aperture height of 0,7. The expected increase in divergence due to temperature changes therefore falls within the error budget generated in section 3.2.2.

If the increase in divergence due to temperature changes would have been too large it could have been reduced by iteratively altering the value of d_2 generated in section 5.2. The thermal dependence of the beam expander could thus be "tuned" to any desired value, provided the divergence deviation is linear with temperature. However, if the divergence is not linear with temperature, the athermalization could only be improved by employing other glasses by trial and error. This non-linearity results as a consequence of the opto-thermal expansion coefficient not being constant within the relevant temperature range.

As is clear for figs. 6.1 - 6.3 the difference between the on-axis and 1mrad field angle angular ray aberrations are very small. This shows that the alignment between the laser and the beam expander is not critical.

The wavefront aberrations of the beam expander at -20, 20 and 60°C are presented graphically in figs 6.4 - 6.6.

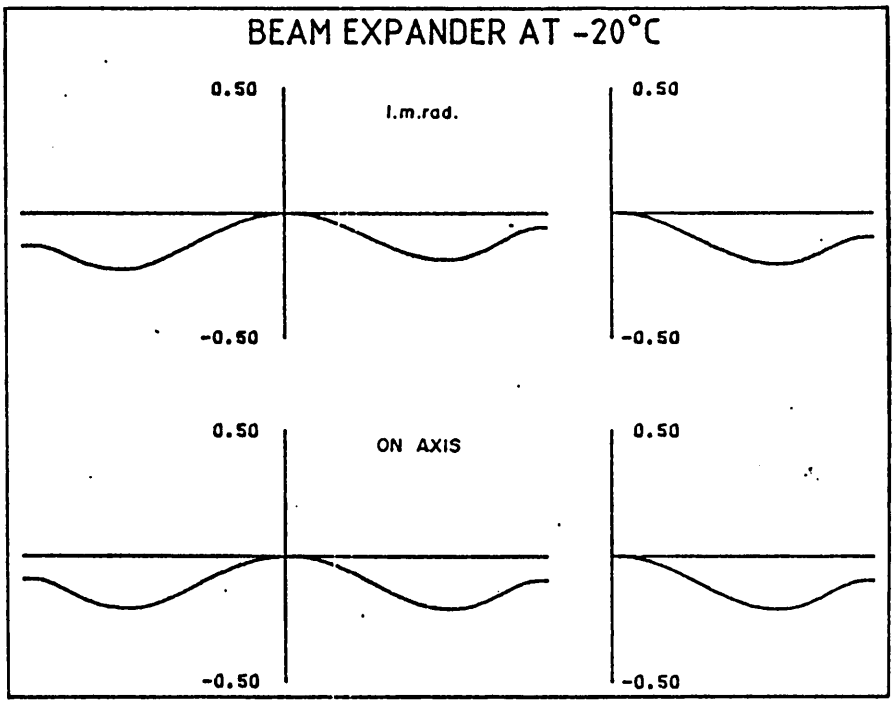

Fig 6.4 Wavefront aberrations in waves

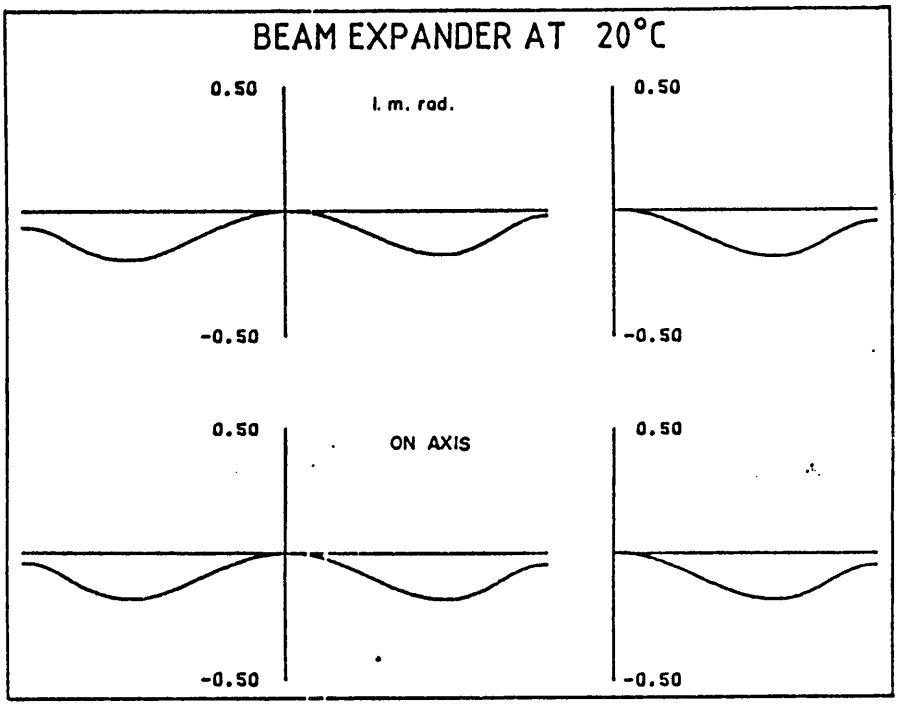

Fig 6.5 Wavefront aberrations in waves

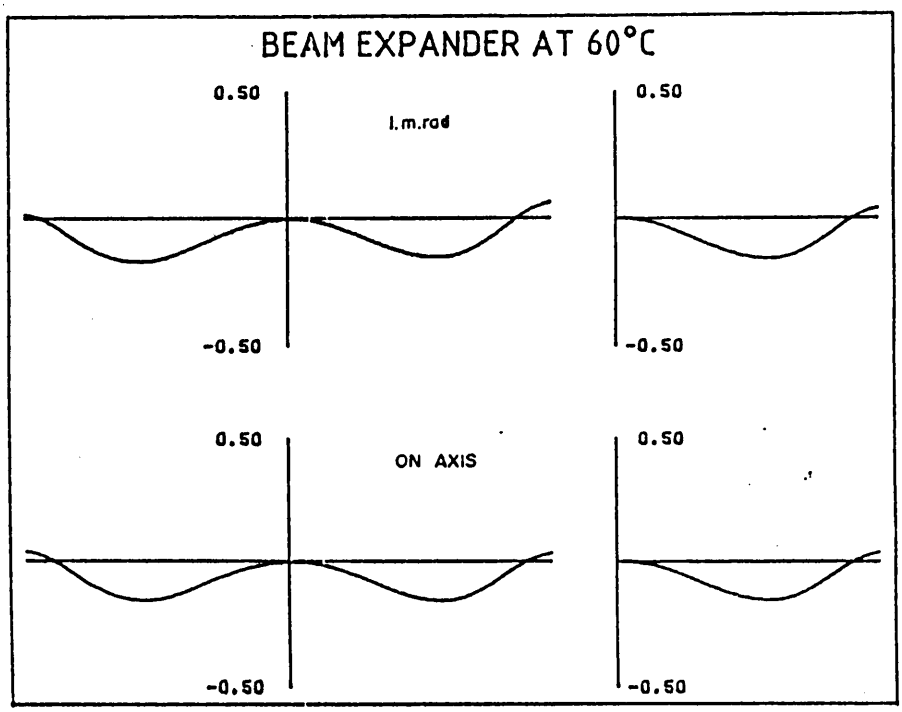

Fig 6.6 Wavefront aberrations in waves

The maximum wavefront error at any temperature or field angle within the relevant ranges is less than a quarter wavelength. This implies that the beam expander is diffraction limited [2].

Since it was shown that the expected increase in divergence as a function of field angle and temperature change is less than 1% of the total divergence, the rest of the evaluation is presented for on-axis points only and at a temperature of 20°C.

6.2 SIMULATION OF THE EXPECTED RADIATION PATTERN.

The expected radiation pattern of the complete system is calculated by convolution of the far-field radiation pattern of the laser with the point spread function (PSF) of the beam expander.

The convolution is done in an indirect way: Firstly the far-field radiation pattern and the PSF are transformed to frequency space by calculating the Fourier transforms of each. These transforms are then multiplied by each other to give the expected radiation pattern in frequency space. This product is then transformed to physical space which gives the expected far-field radiation pattern.

The Fourier transform of the PSF gives the optical transfer function (OTF) of the beam expander. It is thus not necessary to calculate the PSF if the OTF is known.

6.2.1 QUANTIFYING THE OPTICAL PERFORMANCE.

The performance of the beam expander is quantified in term of the optical transfer function (OTF) of the beam expander. The OTF incorporates the degrading effects such as diffraction, aberrations, manufacturing imperfections, apodization and degradation due to temperature effects.

The OTF of an optical system is a complex function and can be decomposed into the modulation transfer function (MTF) and phase transfer function (PTF). The relation between these functions are:

(6.1) $OTF(f) = MTF(f) \exp[PTF(f)]$

where f is the spatial frequency

The PTF of an on-axis beam through a symmetrical optical system is constant due to symmetry. Since the performance of the beam expander is almost identical on-axis and at full field, the PTF of the beam expander is a constant. The performance of the beam expander can thus be uniquely described by the MTF only without loosing any validity.

For the calculation of the system MTF the effect of the near field radiation pattern of the laser was taken into acount by apodizing the pupil of the beam expander with the function given in eq 2.16.

The theoretical MTF of the beam expander is given in table 6.3, where R and T refer to radial and tangential azimuths respectively.

Table 6.3 indicates that the MTF on-axis and at a field angle of 1mrad in object space are almost identical.

TABLE 6.3
Theoretical MTF of the beam expander

Field angle (mrad) Azimuth Spatial frequency(c/mrad)	Theoretical MTF responce 0 R + T	1 R	1 T
5	0,856	0,856	0,856
10	0,628	0,628	0,627
15	0,478	0,478	0,478
20	0,385	0,385	0,385
25	0,284	0,284	0,284
30	0,146	0,146	0,146

The calculation of the MTF is not within the scope of this thesis and was done using existing computer software.

The effect of manufacturing tolerances on the performance of the beam expander was simulated by performing a MTF based tolerance analysis. This analysis gave the expected degradation in MTF as a result of a statistical distribution of the manufacturing tolerances. The degadation in MTF due to a set of manufacturing tolerances is given in table 6.4.

The expected MTF of the system was calculated by subtracting the degradation in MTF from the theoretical MTF.

TABLE 6.4
Theoretical, degradation and expected MTF.

Spatial frequency (c/mrad)	Theoretical MTF	Degradation in MTF	Expected MTF
5	0,856	0,114	0,742
10	0,628	0,250	0,378
15	0,478	0,331	0,147
20	0,385	0,338	0,047
25	0,284	0,271	0,013
30	0,146	0,146	0,000

The resultant MTF was used during the convolution process to simulate the performance of the beam expander.

6.2.2 THE CONVOLUTION.

The reconstruction of the far-field radiation pattern of the complete system was carried out as follows:

a) The frequency content of the object (far field radiation pattern of the laser) was calculated and the frequency spectrum was scaled by the magnification (M = 1/7).

b) The results obtained in (a) were multiplied by the interpolated MTF values of table 6.4

c) The Fourier transform of the product was calculated, which gave the expected far field radiation pattern and divergence of the total system. The

results are presented in table 6.5 and fig 6.8.

TABLE 6.5
Relative intensity of the radiation patterns of the scaled laser and complete system.

Radiation angle (mrad)	Relative intensity Scaled laser divergence	Relative intensity Far-field radiation	Energy within radiation angle
0,00	0,271	0,412	0.0%
0,01	0,306	0,433	0.4%
0,02	0,405	0,492	1.6%
0,03	0,552	0,576	4.0%
0,04	0,720	0,670	7.7%
0,05	0,873	0,752	13.1%
0,06	0,974	0,802	20.3%
0,07	0,998	0,814	29.2%
0,08	0,938	0,777	39.2%
0,09	0,808	0,700	49.8%
0,10	0,638	0,595	60.1%
0,11	0,462	0,477	69.4%
0,12	0,307	0,361	77.5%
0,1356	0,135	-----	-----
0,13	0,187	0,259	83.9%
0,14	0,104	0,177	88.7%
0,15	0,053	0,116	92.2%
0,16	0,025	0,076	94.7%
0,17	0,011	0,046	96.3%
0,18	0,004	0,029	97.4%
0,19	0,002	0,020	98.1%
0,20	0,001	0,014	99.2%

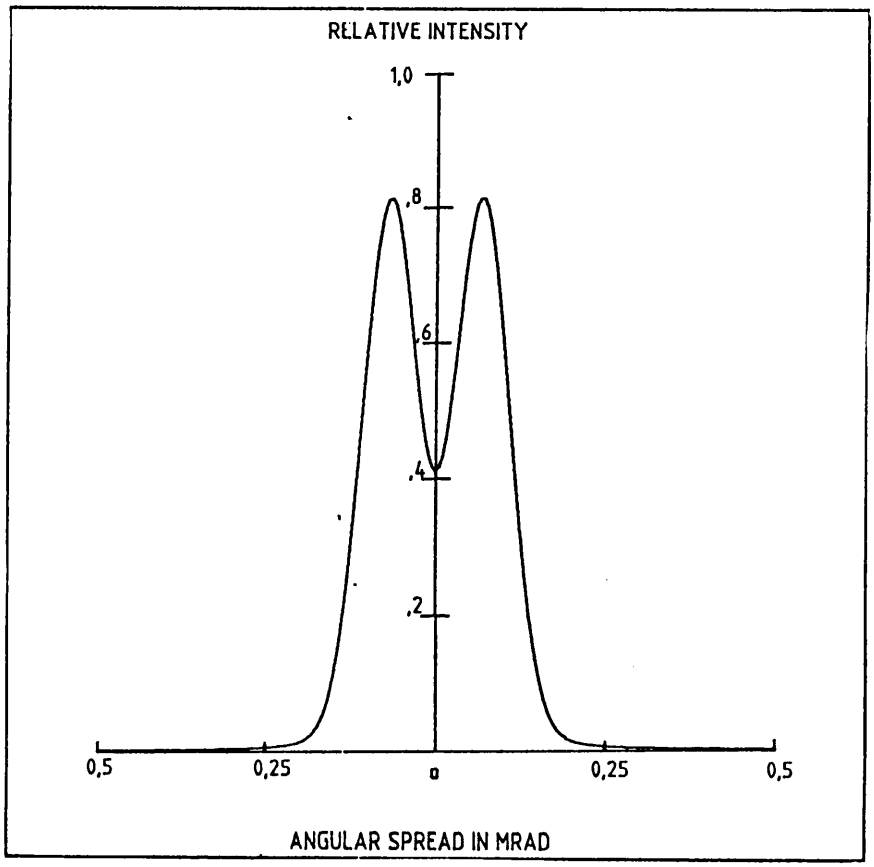

Fig. 6.8 Expected radiation pattern of the complete system

The divergence specification states that the angle subtended by two points opposite sides of the axis where the intensity drops to $1/e^2$ shall be 0,3mrad or less:

The peak intensity of the system is approximately 0,82. Thirteen and a half percent, or $1/e^2$, of the peak intensity is a relative intensity of 0,111. This corresponds to an angle of 0.15mrad according to table 6.5. The divergence of the complete system is thus

expected to be 0,3mrad.

The second divergence specification is that 90% of the laser energy has to be transmitted within the angle of 0,3mrad. Fortunately approximately 92% of the energy is expected to be transmitted into an angle of 0,3mad (refer to table 6.5).

The relative intensity in the centre of the radiation pattern is expected to be 51%. Ideally the relative intensity should be unity. The relative low intensity is a direct consequence of the relative intensity in the centre of the radiation pattern of the laser (refer to fig.2.3). The non-uniformity of the radiation pattern of the laser (which has a relative intensity of 27%) was thus increased by the beam expander. Although the uniformity of the radiation pattern is not a user requirement the relation between the uniformity (or homogeneity) and the first order parameters of the beam expander are derived in the next chapter.

6.3 CONCLUSION

To conclude the evaluation, the beam expander conforms to all of the performance specifications. The total length of the beam expander is 119,39mm and the exit pupil diameter is 49mm. The divergence of the beam expander will not change by more than 1%

from the nominal value within the temperature range of -20 to +60°C.

CHAPTER 7

7 HOMOGENEITY VERSUS USER REQUIREMENTS

The scope of the designs presented in the previous chapters was to a large extent limited by the user specifications. For example, the specifications made it impossible to design a beam expander exhibiting a uniform radiation pattern. For some applications it might be desirable to such a system and in this chapter some systems calculations are presented which relate the degree of uniformity (or homogeneity) of the radiation pattern to the first order parameters of the beam expander. It will also be shown that a homogeneous far-field pattern can be acheived by judicious introduction of aberrations.

7.1 THEORY, DEFINITIONS AND ASSUMPTIONS.

The divergence of the complete laser/beam expander combination for a specific laser is a function of the magnification and the performance of the beam expander. The smaller the magnification and the aberrations of the beam expander, the smaller the divergence will be, and vice versa.

In order to simulate different aberration/magnification

combinations and the resultant degree of uniformity, certain terms have to be quantified:

7.1.1 QUANTIFYING THE PERFORMANCE

The performance of an optical system is a measure of how well the optical information is transfered from object to the image space. This property is quantified by the modulation transfer function (MTF) of the system. An optical system with a low MTF will not have the ability to transfer fine repetitive structures in the object to image space. This shortcoming can be used to achieve a uniform radiation pattern for the beam expander. If, for example, the beam expander had a poor performance, then the two peaks shown in fig. 6.8 could not be imaged and a more uniform radiation pattern for the system would result.
Unfortunately the poor performance will also broaden the pattern shown in fig. 6.8, thereby increasing the divergence of the complete system. This broadening can however be counteracted by decreasing the magnification.

To find the optimum solution, the best balance between aberrations and magnification of the beam expander must be obtained. A simple way to quantify the performance in terms of a single number is the following:

Assume an MTF having the same functional shape as that of the existing design. See fig. 7.1.

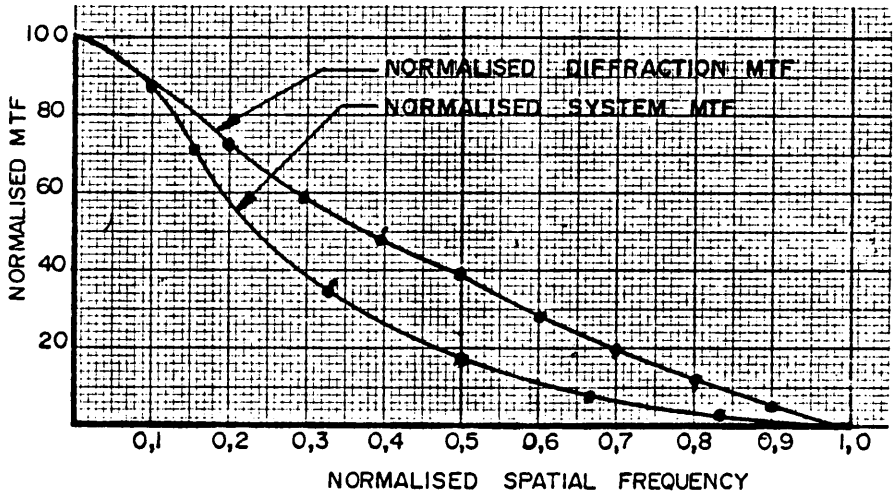

Fig.7.1 Normalised MTF of the existing system and the diffraction limited MTF.

With this assumption the performance can thus be uniquely quantified by the cut-off spatial frequency f' of the system. (The cut-off spatial frequency is the frequency where the modulation is zero).

7.1.2 DEFINITION OF THE HOMOGENEITY.

The homogeneity 'R' of the far-field radiation pattern will be defined as the ratio of the intensity in the centre of

the radiation pattern relative to the maximum intensity.

7.1.3 DEFINITION OF THE DIVERGENCE

The divergence is defined as that angle which is included between those two points on opposite sides of the radiation pattern where the intensity drops to $1/e^2$ of the maximum intensity.

7.2 SIMULATION OF THE DIFFERENT COMBINATIONS.

The homogeneity is a function of the aberration balance and the magnification M. In order to model this function the Fourier transform of the far-field radiation pattern of the laser, which acts as the object of the beam expander, was first of all calculated. This gave the spatial frequency content of the radiation pattern of the laser. The frequency spectrum was then multiplied by the magnification M of the beam expander. This gave the Fourier transform of the far-field radiation pattern assuming a perfect optical system having a magnification M.

The frequency content of the radiation pattern of the complete system was then calculated by multiplying the above result with the expected MTF of the beam expander. The Fourier transform of the product gave the expected far-field radiation pattern of the complete system in real space.

This operation is mathematically equivalent to a convolution of the scaled laser radiation pattern with the point spread function of the beam expander.

This modeling was then carried out for varios magnifications and cut-off spatial frequencies. The combinations which rendered divergences of 0.3mrad are given in table 7.1.

TABLE 7.1

Magnification (M)	Cut-off spatial frequency (f')	Homogeneity (R)	Exit pupil diameter
1/7	31,8	49,0%	49,0
1/7,5	23,9	64,5%	52,5
1/8	19,9	77,3%	56,0
1/8,5	17,6	87,7%	59,5
1/9	15,9	95,3%	63,0
1/9,5	14,6	99,1%	66,5
1/10	13,6	100%	70,0

A large number of simulations were required since no simple mathematical relationship between the magnification M, and cut-off spatial frequency f', which gave divergences of 0.3mrad, exists.

The degree of homogeneity, R, for each combination was then calculated and is given in table 7.1. The exit pupil diameters were also calculated via eq. 3.2 assuming a laser beam diameter of 7mm.

The exit pupil diameters versus the degree of homogeneity R are

presented in fig, 7.2 graph A.

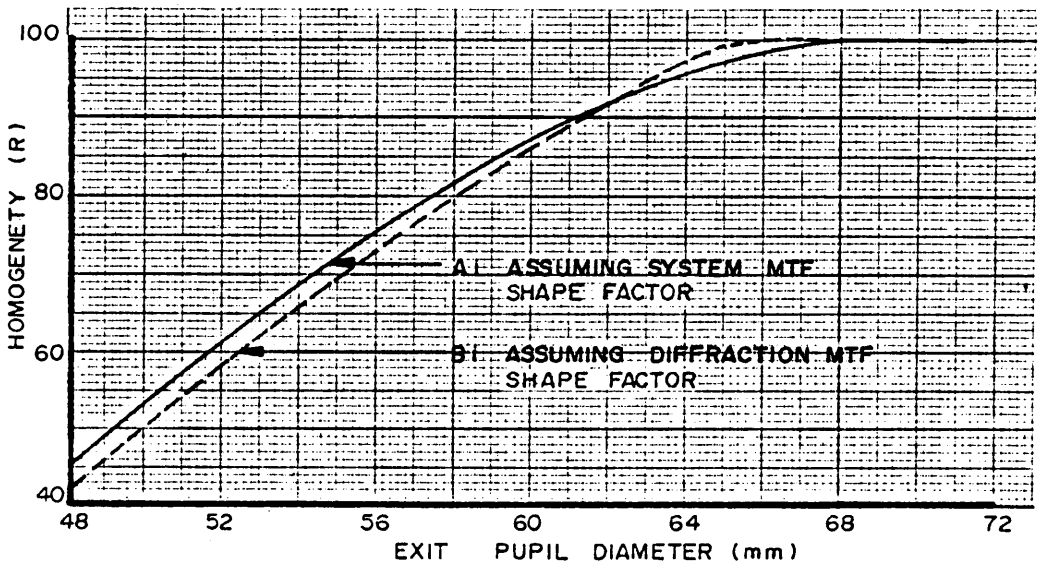

Fig. 7.2 Degree of homogeneity versus exit pupil diameter and MTF shape.

For a given laser system the homogeneity 'R' is a function of the cut-off spatial frequency f', the magnification M, and the MTF shape factor, 'SF'. Of these variables f' and M are the most important. Graph B depicts the relationship between the homogeneity and the exit pupil diameters assuming a shape factor similar to that of the diffraction MTF. As can be seen in fig. 7.2 the homogeneity does not change significantly as a function of MTF shape factors.

7.3 CONCLUSION

If the exit pupil diameter constraint cannot be violated, the homogeneity can not be improved without loosing efficiency. The design presented in chapter 6 would thus be the optimum design. If however a larger exit pupil could be tolerated, the customer can chose a compromise between meeting the exit pupil constraint and having a more homogeneous radiation pattern. Once the customer made his choice, the design will follow along similar lines to the procedures given in chapter 5.

REFERENCES

1. Preussler,D: PART 1` GENERAL SYSTEM DESCRIPTION AND DETAILS OF LASER TRANSMITTER AND COOLING SYSTEM, Optical Sciences Devision, NPRL/CSIR, Pretoria, March 1980.

2. Welford,W.T: ABERRATIONS OF THE SYMMETRICAL OPTICAL SYSTEM, Academic Press, 1974

3. Buchdahl,H.A: AN INTRODUCTION TO HAMILTONIAN OPTICS, Cambridge University Press, 1970

4. Conway,A.W, and Synge,J.L: THE MATHEMATICAL PAPERS OF SIR W.R.HAMILTON, Vol. 1,Cambridge University Press, 1931.

5. Born,M and Wolf,E: PRINCIPLES OF OPTICS, Pergamon Press, London, New York, 1957

6. Smith,W.J: MODERN OPTICAL ENGINEERING, McGraw-Hill Book Company, 1966

7. Kidger,M.J, Image forming systems, APPLIED OPTICS SUMMER COURSE, 30June- 11July 1980, Optics section, Department of Physics, Imperial College of Science and Technology, London SW7 2BZ.

8. Jamieson,T.H, Thermal effects in optical systems, OPTICAL ENGINEERING, March/April 1981, Vol.20, No.2

9. Nortier,F.M: INVESTIGATION OF A CROSSED PORRO-PRISM RESONATOR EMPLOYED IN A Q-SWITHED Nd:Yag LASER, NPRL/CSIR, Pretoria, Feb. 1981

10. Johan Steyl: Private comunication

11. Koechner,W: SOLID STATE LASER ENGINEERING, Springer-Verlag, New York, 1976

12. Gaskill,J.D: LINEAR SYSTEMS, FOURIER TRANSFORMS AND OPTICS, John Wiley & Sons, New York, 1978.

13. Kingslake, LENS DESIGN FUNDAMENTALS, Academic Press, New York, 1978

14. Schott optical glass, GLASSES FOR ATHERMAL OPTICS, Bereich Optik, West Germany

15. Grey,D.S: ATERMALIZATION OF OPTICAL SYSTEMS, Journal of the Optical Society of America, Vol.38, No.6, June 1948

16. Friedman,I: THERMO-OPTICAL ANALYSIS OF TWO LONG-FOCAL-LENGTH AERIAL RECONNAISSANCE LENSES, Optical Engeneering, March/April 1981, Vol.20, No.2

17. Estelle,L.R: THIRD ORDER THEORY OF THERMALLY CONTROLLED PLASTIC AND GLASS TRIPLETS, SPIE, Vol.237, 1980

APPENDIX A

Glass name	Refractive index	αm	dN/dt	αf
BAK50	1,555979	3,7	6,5	-9,7
ZKN7	1,498091	4,5	5,0	-7,4
K51	1,494606	4,3	4,8	-7,3
BASF51	1,703228	5,4	6,7	-5,5
SF11	1,754324	6,1	7,6	-5,2
BASF5	1,587677	7,9	6,6	-5,0
BASF55	1,678316	5,1	5,8	-4,9
BASF52	1,682743	5,2	5,7	-4,6
LAF26	1,725338	5,6	5,6	-3,4
BK3	1,488427	5,3	3,2	-3,2
KZFSN2	1,545474	4,5	3,1	-2,9
SF14	1,733023	6,6	5,9	-2,8
KZFS8	1,697911	5,3	4,6	-2,7
LAFN7	1,726349	5,3	4,8	-2,6
KZFSN5	1,660381	4,8	3,9	-2,6
KZFSN4	1,597248	4,5	3,2	-2,5
KZFSN5	1,635404	4,5	3,4	-2,4
LAF25	1,763196	5,8	5,2	-2,3
LASF13	1,830489	6,2	5,7	-1,8
LAKN16	1,716667	5,3	3,8	-1,3
LASFN3	1,786140	5,9	4,7	-1,3
SK52	1,624905	6,0	3,5	-1,1
SF57	1,811709	8,3	6,5	-0,9
SF13	1,713623	7,1	4,7	-0,8
LAF9	1,766559	7,2	5,2	-0,8
SF6	1,773700	8,1	5,8	-0,6
BALF4	1,567033	6,3	3,0	-0,6
SKN18	1,625003	6,4	3,4	-0,6
SK9	1,601112	6,0	2,9	-0,4
KZF2	1,517168	6,0	2,3	-0,3
LAK28	1,727016	5,7	3,4	-0,3
K10	1,490714	6,5	2,3	-0,1
KZFS6	1,577354	5,1	2,0	-0,0
BK10	1,488213	5,8	1,8	0,1
SK2	1,594852	6,0	2,5	0,2
SK6	1,601056	6,2	2,6	0,3
LASF11	1,781187	5,8	3,3	0,3
BAF9	1,628253	6,5	2,9	0,3
KF50	1,518808	7,3	2,6	0,4
SF54	1,714074	7,7	4,1	0,6
SF4	1,727562	8,0	4,4	0,6
SF10	1,702188	7,5	3,8	0,7
SSK1	1,603963	6,3	2,4	0,7
LAK8	1,697046	5,6	2,4	0,8
LAK10	1,703118	5,7	2,5	0,8

Appendix A

(Cont.)

Glass name	Refractive index	%m	dN/dt	%f
KF9	1,511555	6,8	2,1	0,8
SK5	1,577373	5,5	1,7	0,9
SF8	1,666089	8,2	3,9	0,9
K11	1,490077	6,3	1,7	1,0
SF18	1,696320	8,1	3,9	1,1
SK1	1,597642	6,1	2,0	1,1
SF61	1,723307	7,9	3,9	1,2
SF58	1,876451	9,0	5,8	1,3
SSK2	1,608827	6,2	2,0	1,3
BAF54	1,651055	6,2	2,2	1,3
KZFS1	1,596279	5,0	1,2	1,4
K50	1,511987	7,0	1,9	1,4
LAKN14	1,681527	5,5	1,8	1,4
SF63	1,721103	8,2	3,9	1,4
SSK3	1,601155	6,6	2,1	1,5
BALF6	1,576241	6,7	2,0	1,6
SF55	1,733383	8,2	3,9	1,6
BAF8	1,608946	7,0	2,3	1,6
LAF21	1,769120	5,9	0,3	1,7
SF53	1,702470	8,2	3,6	1,7
BASF54	1,712531	7,3	3,0	1,7
KZF1	1,538215	6,9	1,8	1,8
SF1	1,692485	8,1	3,4	1,8
BAF53	1,653990	6,5	2,1	1,8
SF19	1,645648	7,7	2,8	1,9
LASF15	1,852768	6,3	2,7	2,0
BASF57	1,634406	7,1	2,2	2,1
SF56	1,754630	7,9	3,4	2,1
SF3	1,713406	8,4	3,5	2,1
BAK4	1,556873	7,0	1,7	2,2
SK20	1,548513	6,3	1,3	2,3
BAD5	1,593434	7,6	1,8	2,3
LAK9	1,675805	6,3	1,7	2,4
PSK3	1,541485	6,2	1,1	2,4
SK11	1,552615	6,5	1,3	2,4
SF12	1,628132	7,8	2,4	2,4
K4	1,508060	7,3	1,5	2,4
SF7	1,620278	7,9	2,4	2,5
SF62	1,659181	8,2	2,8	2,5
BASF13	1,678168	7,1	2,1	2,6
SK14	1,591074	6,0	1,0	2,7
SK12	1,571402	6,4	1,1	2,8
BK7	1,506640	7,1	1,2	2,8
F14	1,584197	7,9	2,0	2,8
SSK4	1,604620	6,1	1,1	2,8
PSK2	1,557530	6,4	1,0	2,9

Appendix A

(Cont.)

Glass name	Refractive index	⌀m	dN/dt	⌀f
F5	1,586300	8,0	2,0	2,9
LLF6	1,519204	7,5	1,4	3,0
F9	1,602833	7,7	1,9	3,0
F3	1,595181	8,0	2,0	3,0
PK2	1,508093	6,9	1,0	3,0
RSK52	1,643617	6,7	1,4	3,0
SF15	1,675073	7,9	4,3	3,1
SK19	1,600847	6,4	1,0	3,1
SF5	1,650977	8,2	2,3	3,2
F15	1,588404	8,1	1,9	3,2
BASD56	1,638184	8,1	2,1	3,3
KF3	1,503417	8,1	1,4	3,4
LASF31	1,857243	6,9	2,0	3,4
PK3	1,515146	7,1	0,9	3,5
BASF6	1,650218	7,4	1,5	3,6
SK4	1,600277	6,4	0,7	3,6
BAF3	1,568679	7,8	1,4	3,6
BAK6	1,562392	7,3	0,9	4,0
BAF4	1,590478	7,9	1,3	4,1
FN11	1,602396	7,5	1,1	4,1
SK10	1,609973	7,0	0,8	4,1
SF16	1,626159	8,4	1,7	4,1
SF2	1,627599	8,4	1,7	4,2
F2	1,601841	8,2	1,4	4,3
F6	1,617299	8,5	1,6	4,4
BALKN3	1,508031	7,9	0,8	4,4
SSKN8	1,603545	7,1	0,6	4,5
LAF22	1,759199	7,0	0,9	4,5
SK16	1,607921	6,3	0,1	4,6
LF3	1,566892	8,1	1,0	4,6
F4	1,598587	8,3	1,2	4,7
BK6	1,520571	7,8	0,6	4,8
LLF1	1,534634	8,1	0,8	4,8
BAK1	1,560821	7,6	0,6	4,8
LASF32	1,775915	7,9	1,3	5,0
SK15	1,610256	6,9	0,2	5,0
LASF9	1,822961	7,6	1,1	5,1
BK1	1,500099	7,7	0,3	5,2
BASF1	1,608816	8,5	0,9	5,5
LLF4	1,547452	8,2	0,5	5,5
BAK5	1,545459	7,8	0,2	5,7
SSK51	1,590612	7,6	0,1	5,8
F1	1,607260	8,7	0,8	5,8
BASF10	1,632419	8,6	0,8	5,8
BALF8	1,541213	8,3	0,3	6,0

Appendix A

(Cont.)

Glass name	Refractive infex	⌀m	dN/dt	⌀f
K3	1,507673	8,3	0,2	6,0
BALF51	1,561254	8,1	0,2	6,0
LF1	1,558209	8,5	0,4	6,0
ZK5	1,522509	8,7	0,4	6,1
LF8	1,550103	8,5	0,2	6,4
LAFN3	1,700275	7,8	0,0	6,4
BALF5	1,535596	8,1	-0,1	6,5
LAK21	1,427529	6,8	-0,8	6,5
LF5	1,565879	9,1	0,4	6,7
K5	1,511914	8,2	-0,2	6,7
BAK2	1,529135	8,0	-0,4	6,9
LAK11	1,644477	7,2	-0,8	6,9
K7	1,500865	8,4	-0,3	7,0
BAF52	1,594001	8,4	-0,2	7,1
BAF50	1,665756	8,3	-0,2	7,2
LAKN7	1,638228	7,1	-1,0	7,2
LAFN2	1,725608	8,2	-0,4	7,4
SFN64	1,681547	8,5	-0,3	7,5
BALf50	1,575751	8,3	-0,6	7,7
LAF23	1,673334	8,1	-1,0	8,1
TIF2	1,519432	8,6	-1,2	9,0
LAKN12	1,663589	7,6	-2,0	9,2
SF50	1,633981	10,1	-0,5	9,4
BALK1	1,515906	9,1	-1,3	9,8
PK50	1,511043	8,8	-1,5	9,9
FK3	1,45532*	8,2	-1,8	10,0
LAK23	1,654897	7,9	-2,4	10,1
LAKN13	1,678524	8,4	-2,3	10,4
PSK50	1,547232	8,6	-2,0	10,5
PSK52	1,591855	8,5	-2,2	10,6
SK51	1,608701	8,9	-2,7	11,8
FK5	1,478511	9,2	-2,9	13,3
PSK53	1,608480	9,4	-4,0	14,4
TIK1	1,468772	10,3	-3,9	16,6
LGSK2	1,575239	12,1	-5,0	19,1
FK51	1,479592	13,6	-7,9	28,0
FK54	1,431050	14,6	-7,3	29,3
FK52	1,478921	14,4	-8,2	29,5
PK51	1,520418	13,1	-10,2	30,9